

Accepted Manuscript

Novel 5,6-disubstituted pyrrolo[2,3-*d*]pyrimidine derivatives as broad spectrum antiproliferative agents: Synthesis, cell based assays, kinase profile and molecular docking study

Ju-Hyeon Lee, Ashraf Kareem El-Damasy, Seon Hee Seo, Changdev G. Gadhe, Ae NimPae, Nakcheol Jeong, Soon-Sun Hong, Gyochang Keum

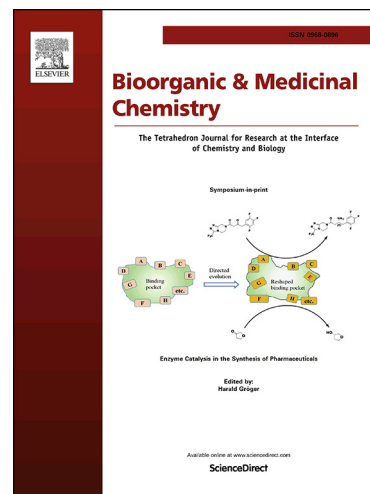
PII: S0968-0896(18)30781-8
DOI: <https://doi.org/10.1016/j.bmc.2018.10.004>
Reference: BMC 14563

To appear in: *Bioorganic & Medicinal Chemistry*

Received Date: 31 May 2018
Revised Date: 1 October 2018
Accepted Date: 7 October 2018

Please cite this article as: Lee, J-H., El-Damasy, A.K., Seo, S.H., Gadhe, C.G., NimPae, A., Jeong, N., Hong, S-S., Keum, G., Novel 5,6-disubstituted pyrrolo[2,3-*d*]pyrimidine derivatives as broad spectrum antiproliferative agents: Synthesis, cell based assays, kinase profile and molecular docking study, *Bioorganic & Medicinal Chemistry* (2018), doi: <https://doi.org/10.1016/j.bmc.2018.10.004>

This is a PDF file of an unedited manuscript that has been accepted for publication. As a service to our customers we are providing this early version of the manuscript. The manuscript will undergo copyediting, typesetting, and review of the resulting proof before it is published in its final form. Please note that during the production process errors may be discovered which could affect the content, and all legal disclaimers that apply to the journal pertain.



Novel 5,6-disubstituted pyrrolo[2,3-*d*]pyrimidine derivatives as broad spectrum antiproliferative agents: Synthesis, cell based assays, kinase profile and molecular docking study

Ju-Hyeon Lee^{a, b, 1}, Ashraf Kareem El-Damasy^{a, c, 1}, Seon Hee Seo^a, Changdev G. Gadhe^d, Ae NimPae^d, Nakcheol Jeong^b, Soon-Sun Hong^{e, *}, Gyochang Keum^{a, *}

^aCenter for Neuro-Medicine, Brain Science Institute, Korea Institute of Science and Technology, Hwarangro 14-gil 5, Seongbuk-gu, Seoul 02792, Korea

^bDepartment of chemistry, Korea University; Anam-ro 145 Seongbuk-gu, Seoul 136-701, South Korea

^cDepartment of Medicinal Chemistry, Faculty of Pharmacy, University of Mansoura, Mansoura 35516, Egypt

^dConvergence Research Center for Diagnosis, Treatment and Care System of Dementia, Korea Institute of Science and Technology, Hwarangro 14-gil 5, Seongbuk-gu, Seoul 02792, Korea

^eDepartment of Drug Development, College of Medicine, Inha University, 3-ga, Sinheung-dong, Jung-gu, Incheon, 400-712, Republic of Korea

¹These authors equally contributed to this work.

*Corresponding authors.

E-mail addresses: gkeum@kist.re.kr (G. Keum), hongs@inha.ac.kr (S.-S. Hong)

Abstract

Two new series of 5-substituted and 5,6-disubstituted pyrrolo[2,3-*d*]pyrimidine octamides (**4a–o** and **5a–m**) and their corresponding free amines **6a–g** and **7a–g** have been synthesized and biologically evaluated for their antiproliferative activity against three human cancer cell lines. The 5,6-disubstituted octamides **6d–g** as well as the amine derivative **7b** have shown the best anticancer activity with single digit micromolar GI₅₀ values over the tested cancer cells, and low cytotoxic effects (GI₅₀ > 10.0 μ M) against HFF-1 normal cell. A structure activity relationship (SAR) study has been established and disclosed that terminal octamide moiety at C2 as well as disubstitution with fluorobenzyl piperazines at C5 and C6 of pyrrolo[2,3-*d*]pyrimidine are the key structural features prerequisite for best antiproliferative activity. Moreover, the most active member **6f** was tested for its antiproliferative activity over a panel of 60 cancer cell lines at NCI, and exhibited distinct broad spectrum anticancer activity with submicromolar GI₅₀ and TGI values over multiple cancer cells. Kinase profile of compound **6f** over 53 oncogenic kinases at 10 μ M showed its highly selective inhibitory activity towards FGFR4, Tie2 and TrkA kinases. The observed activity of **6f** against TrkA (IC₅₀ = 2.25 μ M), FGFR4 (IC₅₀ = 6.71 μ M) and Tie2 (IC₅₀ = 6.84 μ M) was explained by molecular docking study, which also proposed that **6f** may be a type III kinase inhibitor, binding to an allosteric site rather than kinase hinge region. Overall, compound **6f** may serve as a promising anticancer lead compound that could be further optimized for development of potent anticancer agents.

Keywords

Pyrrolo[2,3-*d*]pyrimidine octamides; Mannich reaction; Antiproliferative activity; FGFR4 kinase; Tie2; TrkA; Molecular docking

1. Introduction

Cancer is still one of the most challenging medical problems in the globe, being the second common cause of mortality after cardiovascular diseases [1]. In spite of the enormous research efforts and profound improvements in cancer detection and treatment, accomplishment of optimal cancer therapies is still difficult because of the severe side effects associated with classical cytotoxic chemotherapeutics, as well as emergence of tumor resistance [2]. Over the last two decades, the paradigm of anticancer drug development has been switched significantly from conventional cytotoxic drugs to targeted agents that modulate protein kinases whose activities are more specifically related to cancerous cells. Nowadays, several kinase inhibitors, derived from diverse scaffolds, are being developed in attempt to achieve superior anticancer potency as well as minimal side effects [3]. Pyrrolo[2,3-*d*]pyrimidine, which is most commonly referred to as 7-deazapurine, represents one of the privileged scaffolds for identification of protein kinase inhibitors. A growing body of literature emphasized the interesting antiproliferative activities of various pyrrolo[2,3-*d*]pyrimidine derivatives through inhibition of multiple receptor tyrosine protein kinases, such as epithelial growth factor receptor (EGFR) [4], vascular endothelial growth factor receptor-1 (VEGFR-1) [5], platelet-derived growth factor receptor- β (PDGFR- β) [4, 6–8], and insulin-like growth factor receptor (IGFR) [9, 10] (Figure 1). Moreover, certain non-receptor tyrosine protein kinases were potently inhibited by pyrrolo[2,3-*d*]pyrimidines (Figure 1). For example, Yoriko *et al.* discovered RK-20449, a pyrrolo[2,3-*d*]pyrimidine member, as a potent hematopoietic cell kinase (HCK) for treatment of leukemia [11]. Recently, Francesca *et al.* reported the selective Src kinase inhibitory activity of certain pyrrolo[2,3-*d*]pyrimidines *in vitro* active against glioblastoma [12].

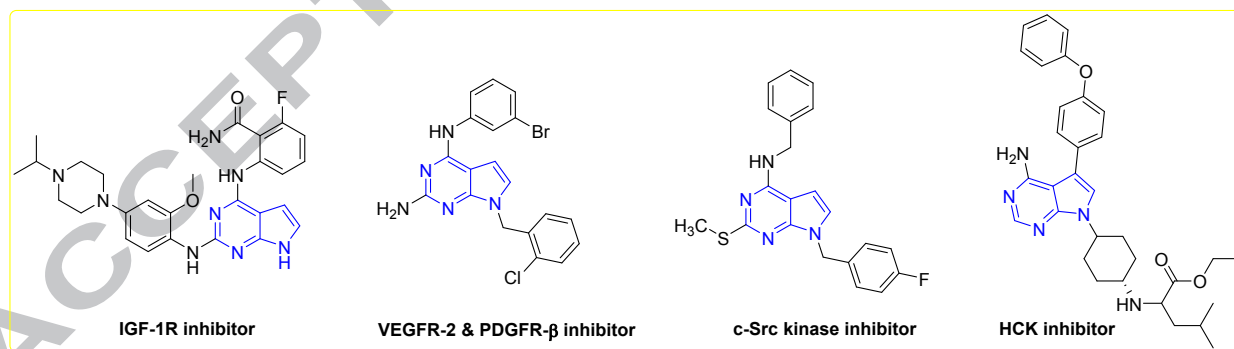


Figure 1. Representative examples of antiproliferative pyrrolo[2,3-*d*]pyrimidine derivatives with protein kinase inhibitory activities.

On the other hand, Mannich bases, the products of classical Mannich reaction, constitute a substantial class of compounds found in several anticancer chemotherapeutics [13]. Mannich bases or aminoalkyl derivatives of indoles, bioisostere of pyrrolopyrimidine, and other bicyclic ring systems exhibited potent cytotoxic activities against various cancer cell lines through different mechanisms of action, like induction of apoptosis [14], inhibition of isoprenylcysteine carboxyl methyltransferase (Imct)

[15], or inhibition of certain oncogenic kinases (VEGFR and PDGFR) [16] and phosphatidylinositol-3-kinase α (PI3K α) inhibitors [17] (Figure 2).

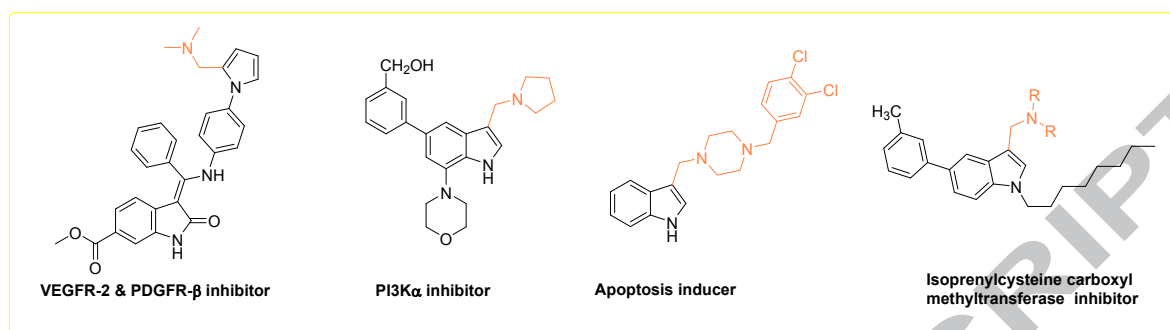


Figure 2. Certain reported Mannich bases with promising antiproliferative activities. The aminoalkyl moiety is illustrated in orange. Despite of the extensive investigation of pyrrolopyrimidines as antiproliferative agents, only few Mannich bases of pyrrolopyrimidine were reported to date, and none of them was examined for its anticancer activity so far. In view of the aforementioned considerations, and in pursuit of our ongoing endeavors to identify new potent antiproliferative agents [18–24], four new series of pyrrolopyrimidine Mannich bases; **4a–o**, **5a–m** and their corresponding free amines **6a–g** and **7a–g** have been synthesized for the first time (Figure 3). The antiproliferative activities of the target compounds were examined against a panel of three human cancer cell lines; HCT-116 colorectal carcinoma and MCF-7 and SK-BR3 breast cancer cells. Moreover, the kinase inhibitory activity for the most potent derivative, compound **6b**, was also profiled to investigate the potential mechanism of action at molecular level.

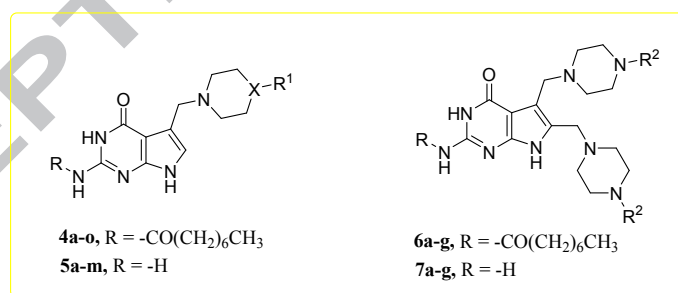


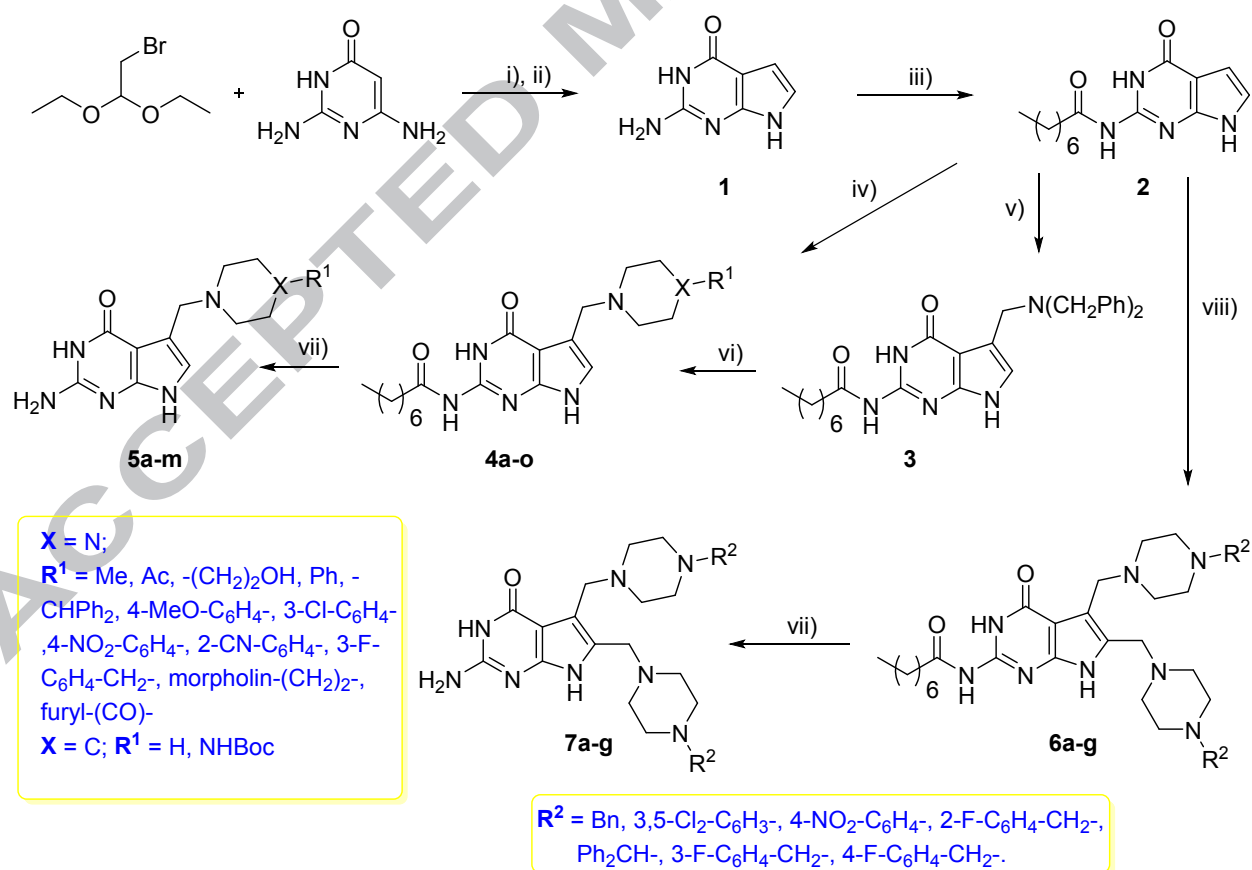
Figure 3. General structure of the target compounds.

2. Results and discussion

2.1. Chemistry

As shown in Scheme 1, the main starting material **1** was prepared *via* treatment of bromoacetaldehyde diethyl acetal with HCl and sodium acetate, then cyclization with 2,6-diamino-4-pyrimidinone [25]. Since pyrrole ring of compound **1** possesses three active protons (C5-H, C6-H, and NH) with different reactivity towards the proposed Mannich reaction, we adopted the protection of amino group in attempt to selectively achieve monosubstitution at C5 of pyrrolo[2,3-*d*]pyrimidine [26]. Therefore, compound **1** was reacted with octanoyl chloride in pyridine to furnish the key intermediate

pyrrolo[2,3-*d*]pyrimidin-2-yl octamide (**2**) in 75% yield [26]. The corresponding 5-monosubstituted pyrrolopyrimidines **3**, **4a–f**, and **4n** were generated through Mannich-type reaction of compound **2** with *N,N*-dibenzylamine or the proper arylpiperazine or piperidine, and 80% aqueous formaldehyde in acidic conditions [26]. It is noteworthy mentioning that upon completion of Mannich-type reaction, the reaction mixture was subjected to acidic treatment with 0.5 M aqueous HCl to cleave the undesired *N*-alkylated product and afford only C-alkylated derivative. Despite of the octanoyl protection of amine group in compound **2**, the highly electron deficient aryl or benzyl piperazines provided 5,6-disubstituted pyrrolo[2,3-*d*]pyrimidin-2-yl octamides **6a–g** under the same reaction conditions. Upon using 1-benzylpiperazine, a mixture of mono and disubstituted pyrrolo[2,3-*d*]pyrimidine octamides, **4b** and **6a**, was formed in 61% and 10% yield, respectively. Also, a mixture of mono and disubstituted derivatives, **4f** and **6c**, was obtained in 48% and 52% yield, respectively, when using 4-nitrophenyl piperazine. In order to solely get the 5-monosubstituted derivatives **4g–m** and **4o**, we introduced amine-exchange reaction with compound **3** in MeOH/THF (1/1) in a sealed tube at 75°C. Amide hydrolysis of compounds **4a–o** and **6a–g** was performed under basic conditions [26] with KOH for 72 h to afford the corresponding 2-amino derivatives **5a–m** and **7a–g** in excellent yields (Scheme 1).



Scheme 1. Reagents and reaction conditions: i) conc. HCl, NaOAc, 90 °C to rt, ii) 2,6-Diamino-4-pyrimidinone, NaOAc, 80 °C to rt, quant.; iii) Octanoyl chloride, pyridine, 85 °C, 49–75%; iv) 37% formalin, aryl piperazine, 80% AcOH, 75 °C, 12%–quant.; v) 37% Formalin, *N,N*-dibenzylamine,

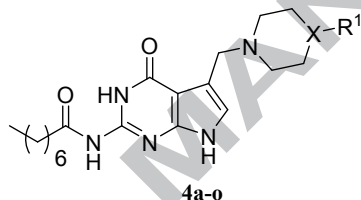
80% AcOH, 75 °C, 24–74%; vi) Appropriate amines, MeOH/THF (1:1), 75 °C, 11–97%; vii) 5 M aq. KOH, MeOH/THF, rt, 60%–quant.; viii) 37% Formalin, aryl or benzyl piperazine, 80% acetic acid, 75 °C, 9%–quant.

2.2. In vitro screening of the antiproliferative activities.

2.2.1. Preliminary evaluation against three human cancer cell lines

All final compounds **4a–o**, **5a–m**, **6a–g**, and **7a–g** were preliminary evaluated for their antiproliferative activity at 10 μM concentration against three human cancer cell lines, HCT-116 (human colorectal carcinoma) and MCF-7 and SK-BR3 (breast cancer cells), by MTT assay method and BIIB021 was used as a reference compound. The percentages of growth inhibition (GI) as well as GI₅₀ of compounds **4a–o** against the three cell lines are listed in Table 1. The compound was considered active if it achieves GI > 65% and/or GI₅₀ < 8.0 μM.

Table 1. In vitro growth inhibitory data of the 5-substituted pyrrolopyrimidinyl octamides **4a–o** against MCF-7, SK-BR-3 and HCT116 cancer cell lines.

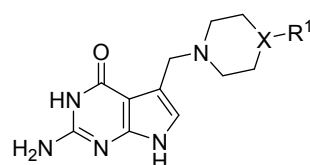


Compound No.	X	R ¹	MCF-7		SKBR3		HCT116	
			% GI ^a	GI ₅₀ ^b	% GI ^a	GI ₅₀ ^b	% GI ^a	GI ₅₀ ^b
4a	N	C ₆ H ₅ -	50.26	-	67.56	0.63 ± 0.03	73.90	3.99 ± 0.82
4b	N	(C ₆ H ₅) ₂ -CH-	58.43	-	67.41	0.41 ± 0.12	75.47	1.01 ± 0.23
4c	N	4-CH ₃ O-C ₆ H ₄ -	49.19	-	71.36	1.23 ± 0.11	71.44	8.94 ± 2.63
4d	N	3-Cl-C ₆ H ₄ -	43.40	-	69.69	0.95 ± 0.06	72.73	7.17 ± 3.00
4e	N	2-CN-C ₆ H ₄ -	59.21	-	84.61	0.97 ± 0.16	79.52	1.46 ± 0.13
4f	N	4-NO ₂ -C ₆ H ₄ -	40.37	-	61.61	8.04 ± 1.45	68.47	-
4g	N	3-F-C ₆ H ₄ -CH ₂ -	85.74	7.84 ± 0.65	91.18	5.58 ± 0.72	92.83	5.34 ± 0.59
4h	N	CH ₃ -	59.56	-	50.36	-	51.02	-
4i	-	imidazole-	68.17	-	86.09	-	80.48	-
4j	N	CH ₃ (C=O)-	35.78	-	40.25	-	43.83	-
4k	N	2-furyl-(C=O)-	68.54	-	71.16	-	60.20	-
4l	N	HOCH ₂ CH ₂ -	41.99	-	62.16	-	67.29	-
4m	N	Morpholin-CH ₂ CH ₂ -	88.56	-	90.36	-	93.05	-
4n	C	H	70.21	13.43 ± 2.64	77.13	15.04 ± 5.44	51.06	14.90 ± 4.22
4o	C	(CH ₃) ₃ CO(C=O)NH-	36.45	-	59.32	-	50.28	-
BIIB021	-	-	84.81	0.392±0.03	71.94	0.347±0.023	86.20	0.227±0.015

^a% Growth inhibition values were obtained using MTT assay at 10 μM concentration after incubation for 72 hours, and the bold figures refer to %GI > 65. ^bIC₅₀ values (±SD) were obtained from the dose-response curve. ^c Not determined.

Close examination of the results revealed that the piperazine derivatives (**4a–m**) generally possess superior antiproliferative activities to piperidines **4n** and **4o**. On the terminal nitrogen of piperazine, various structural fragments were attached for exploration of their anticancer activities. Direct installation of phenyl (**4a**) or substituted phenyl (**4c–f**) was found to be favorable for activity. The phenyl piperazine derivative **4a** exerted remarkable antiproliferative activity ($GI_{50} = 0.63 \pm 0.03 \mu\text{M}$) against SKBR3 cell line and moderate activity ($GI_{50} = 3.99 \pm 0.82 \mu\text{M}$) against HCT116 cell line. Substitution of phenyl piperazine with electron withdrawing chlorine or cyano group is tolerable for retaining the activity (**4d**, $GI_{50} = 0.95 \pm 0.06 \mu\text{M}$; **4e**, $GI_{50} = 0.97 \pm 0.16 \mu\text{M}$) against SKBR3, while introduction of *p*-nitro group greatly reduced the antiproliferative activity (**4f**, $GI_{50} = 8.04 \pm 1.45 \mu\text{M}$) against SKBR3. Furthermore, installation of *p*-methoxy moiety as electron donating group led to two folds drop in activity (**4c**, $GI_{50} = 1.23 \pm 0.11 \mu\text{M}$) against SKBR3. Replacement of phenylpiperazine with 1-benzylpiperazine improved the activity (**4b**, SKBR3, $GI_{50} = 0.41 \pm 0.12 \mu\text{M}$; HCT116, $GI_{50} = 1.01 \pm 0.23 \mu\text{M}$). Interestingly, introduction of *m*-fluorobenzyl moiety broaden the spectrum of antiproliferative activity to include MCF7 cell line with moderate potency (**4g**, $GI_{50} = 5.34\text{--}7.84 \mu\text{M}$). Replacing the bulky phenyl group with small lipophilic methyl (**4h**) or acetyl (**4j**) decreased the activity, while insertion of hydrophilic imidazole ring (**4i**) or 2-morpholinoethyl (**4m**) was favorable for the anticancer activity (**4i**, %GI = 68.17–86.09; **4m**, %GI = 88.65–93.05). In contrast to the promising activity of several octamide derivatives, their corresponding free amines **5a–m** showed modest antiproliferative activity (Table 2). This superiority of octamides than amines may be attributed to the increase in compound lipophilicity, permeability and penetration into cancer cells and thus the cellular potency. Relatively, the *m*-chlorophenyl piperazine derivative **5d** is the best in this series with compounds with GI_{50} values of $8.28 \pm 1.37 \mu\text{M}$ and $7.66 \pm 1.05 \mu\text{M}$ against SKBR3 and HCT116 cell lines, respectively.

Table 2. *In vitro* growth inhibitory data of the 2-amino-5-substituted pyrrolopyrimidinones **5a–m** against MCF-7, SK-BR-3 and HCT116 cancer cell lines.



5a-m

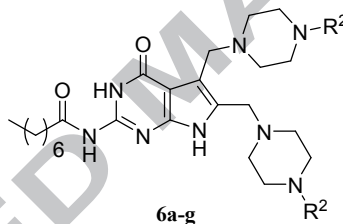
Compound No.	X	R ¹	MCF-7		SKBR3		HCT116	
			% GI ^a	GI ₅₀ ^b	% GI ^a	GI ₅₀ ^b	% GI ^a	GI ₅₀ ^b
5a	N	C ₆ H ₅ -	49.73	-	30.71	-	48.97	-
5b	N	(C ₆ H ₅) ₂ -CH-	79.55	33.89 ± 1.59	4.22	-	80.45	20.27 ± 2.26
5c	N	4-CH ₃ O-C ₆ H ₄ -	51.73	-	57.48	11.17 ± 1.55	69.22	-
5d	N	3-Cl-C ₆ H ₄ -	54.23	-	67.46	8.28 ± 1.37	79.29	7.66 ± 1.05
5e	N	2-CN-C ₆ H ₄ -	51.08	-	73.79	23.7 ± 1.26	71.97	8.37 ± 1.22

5f	N	4-NO ₂ -C ₆ H ₄ -	26.81	- ^c	27.50	- ^c	28.54	- ^c
5g	N	3-F-C ₆ H ₄ -CH ₂ -	20.62	- ^c	16.80	- ^c	31.12	- ^c
5h	N	CH ₃ -	20.21	- ^c	28.96	- ^c	16.48	- ^c
5i	-	imidazole-	38.76	- ^c	38.84	- ^c	50.64	- ^c
5j	N	CH ₃ (C=O)-	16.21	- ^c	24.21	- ^c	13.81	- ^c
5k	N	HOCH ₂ CH ₂ -	18.80	- ^c	32.84	- ^c	17.82	- ^c
5l	N	morpholin- CH ₂ CH ₂ -	19.46	- ^c	27.11	- ^c	15.40	- ^c
5m	C	H-	23.76	- ^c	17.50	- ^c	24.13	- ^c
BIIB021	N	-	84.81	0.392±0.03	71.94	0.347±0.023	86.20	0.227±0.015

^a % Growth inhibition values were obtained using MTT assay at 10 μ M concentration after incubation for 72 hours, and the bold figures refer to %GI > 65. ^b IC₅₀ values (\pm SD) were obtained from the dose-response curve. ^c Not determined.

Regarding the 5,6-disubstituted pyrrolopyrimidinyl octamides **6a–g** and their amino derivatives **7a–g**, their antiproliferative activities are shown in Table 3 and Table 4, respectively.

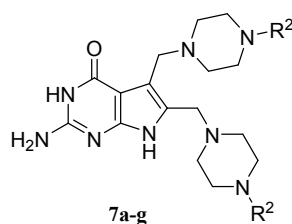
Table 3. *In vitro* growth inhibitory data of the 5,6-Bis-substituted pyrrolopyrimidinyl octamides **6a–g** against MCF-7, SK-BR-3 and HCT116 cancer cell lines.



Compound No.	R ²	MCF-7		SKBR3		HCT116	
		% GI ^a	GI ₅₀ ^b	% GI ^a	GI ₅₀ ^b	% GI ^a	GI ₅₀ ^b
6a	(C ₆ H ₅) ₂ -CH-	15.16	- ^c	67.33	6.43 \pm 0.22	41.53	18.38 \pm 4.80
6b	3,5-Cl ₂ -C ₆ H ₃ -	10.70	- ^c	42.54	- ^c	6.88	- ^c
6c	4-NO ₂ -C ₆ H ₄ -	12.56	- ^c	64.59	- ^c	27.04	- ^c
6d	C ₆ H ₅ -CH ₂ -	96.57	2.78 \pm 0.01	93.40	3.64 \pm 0.03	97.01	4.09 \pm 0.03
6e	2-F-C ₆ H ₄ - CH ₂ -	96.13	4.20 \pm 0.03	93.39	3.73 \pm 0.06	97.28	1.89 \pm 0.30
6f	3-F-C ₆ H ₄ - CH ₂ -	94.76	2.15 \pm 0.09	93.06	3.91 \pm 0.34	95.54	2.25 \pm 0.12
6g	4-F-C ₆ H ₄ - CH ₂ -	97.23	1.75 \pm 0.15	93.52	3.60 \pm 0.06	97.14	4.13 \pm 0.15
BIIB021	-	84.81	0.392 \pm 0.03	71.94	0.347 \pm 0.023	86.20	0.227 \pm 0.015

^a % Growth inhibition values were obtained using MTT assay at 10 μ M concentration after incubation for 72 hours, and the bold figures refer to %GI > 65. ^b IC₅₀ values (\pm SD) were obtained from the dose-response curve. ^c Not determined.

Table 4. *In vitro* growth inhibitory data of the 2-Amino-5,6-bis-substituted pyrrolopyrimidinones **7a–g** against MCF-7, SK-BR-3 and HCT116 cancer cell lines.



Compound No.	R ²	MCF-7		SKBR3		HCT116	
		% GI ^a	GI ₅₀ ^b	% GI ^a	GI ₅₀ ^b	% GI ^a	GI ₅₀ ^b
7a	(C ₆ H ₅) ₂ -CH-	13.77	- ^c	11.08	- ^c	10.69	- ^c
7b	3,5-Cl ₂ -C ₆ H ₃ -	82.46	4.02 ± 0.53	90.03	3.22 ± 0.14	91.73	2.89 ± 0.13
7c	4-NO ₂ -C ₆ H ₄ -	1.26	- ^c	6.79	- ^c	1.94	- ^c
7d	C ₆ H ₅ -CH ₂ -	21.19	- ^c	15.69	- ^c	21.36	- ^c
7e	2-F-C ₆ H ₄ - CH ₂ -	8.91	- ^c	58.96	- ^c	12.80	- ^c
7f	3-F-C ₆ H ₄ - CH ₂ -	16.08	- ^c	10.50	- ^c	13.59	- ^c
7g	4-F-C ₆ H ₄ - CH ₂ -	18.36	- ^c	23.21	- ^c	22.97	- ^c
BIIB021	-	84.81	0.392 ± 0.03	71.94	0.347 ± 0.023	86.20	0.227 ± 0.015

^a % Growth inhibition values were obtained using MTT assay at 10 μ M concentration after incubation for 72 hours, and the bold figures refer to %GI > 65. ^b IC₅₀ values (\pm SD) were obtained from the dose-response curve. ^c Not determined.

As revealed from the results listed in Table 3, the benzylpiperazine derivatives **6d–g** exerted superior antiproliferative activities to phenyl piperazines **6a–c**. In this set of compounds, compound **6f** was found to be the most potent member with GI₅₀ values of 2.15 \pm 0.09 μ M, 3.91 \pm 0.34 μ M and 2.25 \pm 0.12 μ M against MCF7, SKBR3 and HCT116 cell lines, respectively. Upon comparing **6f** with its relevant monosubstituted derivative **4g**, it could be observed that disubstitution is more auspicious for the antineoplastic activity. Compounds **6e** and **6g**, the positional isomers of **6f**, exhibited comparable activity (marginally superior or inferior) to the unsubstituted benzyl piperazine **6d**. As expected, **7a–g**, the corresponding amino derivatives of **6a–g**, showed weak growth inhibitory activities against the three tested cancer cell lines. The only exception was the 3,5-dichlorophenyl piperazine derivative **7b**, which displayed reasonable activity with GI₅₀ values of 4.02 \pm 0.53 μ M, 3.22 \pm 0.14 μ M and 2.89 \pm 0.13 μ M against MCF7, SKBR3 and HCT116 cell lines, respectively.

2.2.2. In vitro antiproliferative activities against NCI-60 cell line panel

2.2.2.1. Single dose testing

Prompted by the promising preliminary antiproliferative activity and in order to interrogate the antiproliferative activity of the target compounds on broad extent, compounds **6f** and **7b** as representative examples were submitted to National Cancer Institute (NCI, Bethesda, Maryland, USA) [27] for appraisal of their antiproliferative activities against clinically important cancer cell lines. According to the NCI protocol, compounds **6f** and **7b** were tested at a single dose concentration of 10 μ M over a panel of approximately 60 human cancer cell lines comprising nine human cancer

cell types; leukemia, non-small cell lung, colon, central nervous system, melanoma, ovarian, renal, prostate, and breast tumor cell lines. The growth percentages of all tested cell lines after treatment with the tested compounds are illustrated in Figure 4.

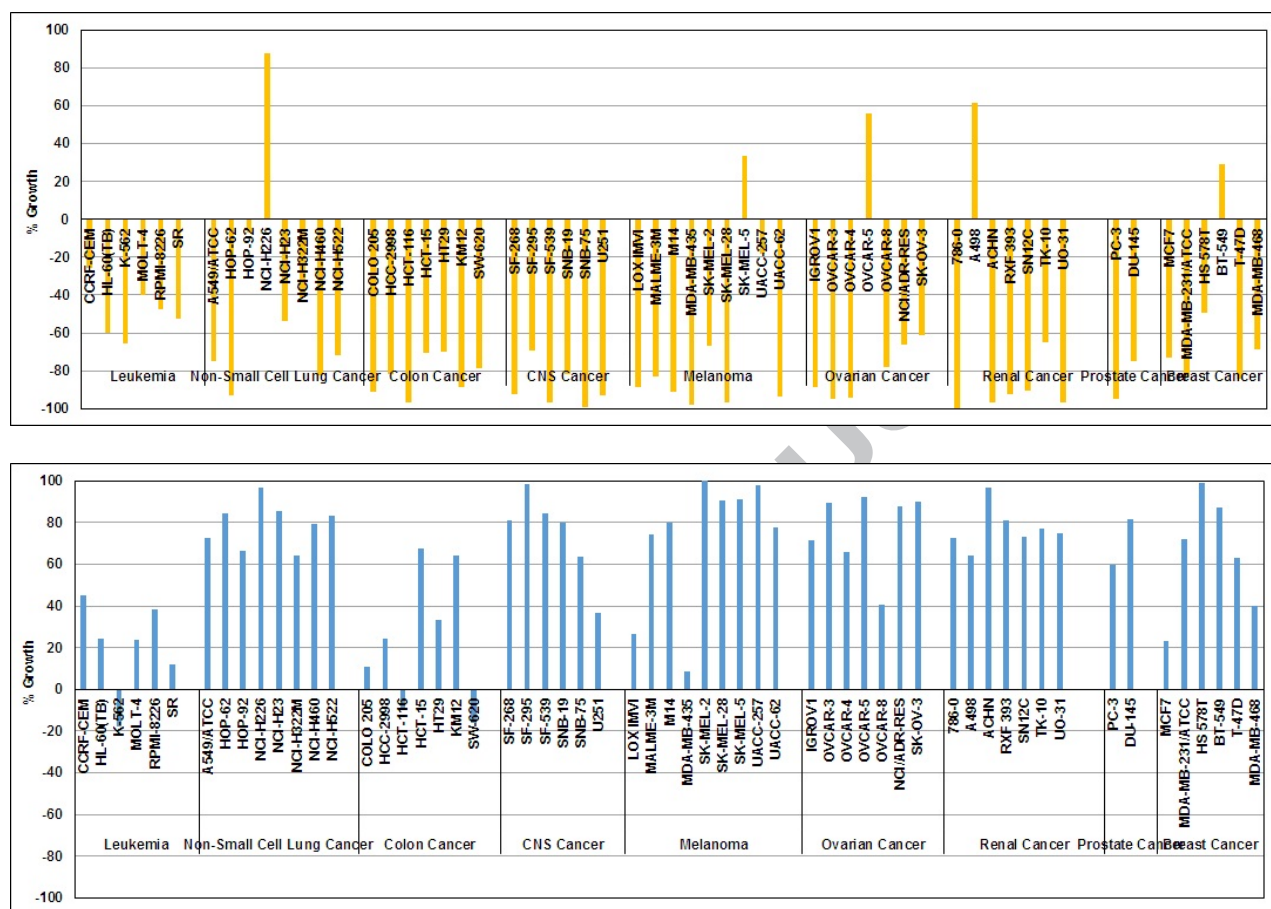


Figure 4. % Growth of NCI 60 cell line panel upon treatment with compounds **6f** (upper panel) and **7b** (lower panel) at 10 μ M concentration.

Close inspection of the results presented in Figure 4, demonstrated the broad spectrum antiproliferative activity of compound **6f** over all the nine examined cancer types. Compound **6f** exerted distinct cytotoxic effects (minus % growth) against 52 cell lines out of 56. Of particular importance, compound **6f** displayed lethal activity over HCT-116 (colon cancer), SF-539 (CNS cancer), SK-MEL-28 (melanoma), and the renal carcinoma cells ACHN and UO-31 with percentages growth values of -96.68% , -96.93% , -96.98% , -96.57% and -96.54% , respectively. In contrast to the broad spectrum cytotoxic activity of **6f**, the pyrrolopyrimidine 2-amine derivative **7b** manifested good cytostatic effect (% growth < 40) with limited spectrum of activity against 14 cancer cell lines derived from leukemia, melanoma, colon and breast cancer types. Such finding further emphasizes the essential role of octamide moiety for achieving the favorable antiproliferative activity.

2.2.2.2. Five-dose testing

Compounds **6f** and **7b** satisfied the criteria set by NCI for activity in the preliminary assay and consequently they were further tested in a five-dose testing mode at 10-fold dilution (100–0.01 μ M) over the full panel. Three response parameters were determined for each compound; GI_{50} (the

concentration producing 50% growth inhibition, a measure of compound's potency), TGI (the concentration producing 100% growth inhibition, a measure of compound's efficacy) and LC₅₀ (the concentration causing 50% lethality, a measure of compound's cytotoxicity and efficacy). The GI₅₀ values of compounds **6f** and **7b** are showed in Table 5.

Table 5. GI₅₀ values (μ M) of compounds **6f** and **7b** over NCI-60 cell line panel.^{a,b}

	Cancer type/ Cell line	6f	7b		Cancer type/ Cell line	6f	7b
Leukemia	CCRF-CEM	0.25	2.07	Melanoma	MDA-MB-435	0.32	1.62
	HL-60(TB)	1.74	- ^b		SK-MEL-2	- ^b	2.21
	K-562	0.21	2.33		SK-MEL-28	- ^b	1.79
	MOLT-4	0.26	2.58		SK-MEL-5	1.57	1.63
	RPMI-8226	0.36	2.41		UACC-257	0.20	2.06
	SR	0.21	1.46		UACC-62	1.68	1.8
	A549/ATCC	0.34	1.82		IGROV1	1.43	1.95
Non-Small Cell Lung Cancer	HOP-62	1.42	1.67	OVCAR-3	0.78	1.81	
	HOP-92	1.14	1.35	OVCAR-4	1.21	1.58	
	NCI-H226	1.84	15.8	OVCAR-5	- ^b	2.64	
	NCI-H23	1.86	2.03	OVCAR-8	0.21	2.05	
	NCI-H322M	1.46	6.33	NCI/ADR-RES	1.5	>100	
	NCI-H460	0.38	1.96	SK-OV-3	1.9	4.62	
	NCI-H522	1.91	1.74	786-0	1.54	1.57	
Colon Cancer	COLO 205	1.4	1.69	A498	1.25	1.69	
	HCC-2998	0.25	1.7	ACHN	- ^b	1.94	
	HCT-116	0.17	1.63	CAKI-1	1.32	5.1	
	HCT-15	0.30	1.93	RXF 393	0.51	1.58	
	HT29	0.26	1.74	SN12C	1.48	1.91	
	KM12	0.72	1.83	TK-10	1.74	1.8	
	SW-620	0.19	1.72	UO-31	0.38	11.7	
CNS Cancer	SF-268	1.26	1.77	PC-3	1.3	1.76	
	SF-295	1.41	1.82	DU-145	1.1	1.92	
	SF-539	- ^b	1.72	MCF7	0.19	1.58	
	SNB-19	1.56	1.77	MDA-MB-231/ATCC	0.59	2.01	
	SNB-75	1.34	1.42	HS 578T	1.72	1.78	
	U251	0.17	1.67	BT-549	1.53	1.72	
	LOX IMVI	0.20	1.94	T-47D	1.6	1.78	
Melanoma	MALME-3M	0.67	2.00	MDA-MB-468	0.48	1.72	
	M14	0.21	1.83				

^a Bold figures refer to sub-micromolar GI₅₀ values.

^b NT: not tested, ^c ND: not determined

As illustrated in Table 5, the fluoro substituted pyrrolopyrimidine octamide **6f** showed high potency with sub-micromolar or one-digit micromolar (less than 2.0 μ M) GI₅₀ values over 26 and 24 cell lines, respectively. Leukemia, colon cancer and melanoma were found to be the most sensitive types of cancer responsive to compound **6f**. It showed equipotent activity towards CCRF-CEM and PRMI-8226 leukemia cells and HCC-2998 and HT29 colon cancer cell lines with GI₅₀ value of 260 nM. Moreover, compound **6f** strongly suppressed the proliferation of LOX IMVI, M14 and UACC-257 melanoma cell lines with GI₅₀ value of 200 nM. Besides the previously mentioned targeted cellular

potencies of compound **6f**, it exhibited significant broad spectrum antiproliferative activity over other multiple cell lines such as U251CNS cancer, OVCAR-8 ovarian cancer, and MCF7 breast cancer cell lines with GI_{50} values of 0.17, 0.21 and 0.19 μM , respectively. On the other hand, the pyrrolopyrimidine 2-amine derivative **7b** exerted remarkable antiproliferative activity (mean GI_{50} value = 1.8 μM) against most of the tested cell lines, yet with inferior potency when compared with compound **6f**. It was evident that the octamide derivative **6f** is more potent than the free amine compound **7b** regarding most of the cell lines, particularly leukemia, colon cancer and leukemia. Such conclusion implies the significance of octamide side chain for antiproliferative activity of this new series of compounds.

In view of the efficacy related parameters (TGI and LC_{50} values) of compounds **6f** and **7b** (Table 6), it is obvious that compound **6f** is also more efficacious than **7b** towards most of the examined cell lines. Compound **6f** completely inhibited the proliferation of several cancer cells at submicromolar concentrations, with about 10 times superiority than compound **7b**. For instance, **6f** exerted TGI values of 0.32, 0.42, and 0.55 μM against HCT-116 colon cancer cell, LOX IMVI melanoma cell, and K-562 leukemia cell line, respectively. In terms of LC_{50} values, both compounds **6f** and **7b** showed limited efficacy against leukemia cell lines with LC_{50} more than 100 μM . Upon considering both TGI and LC_{50} values, it was observed that compound **6f** exerted remarkable efficacies against HCT-116 colon cancer cell, U251 CNS cancer, LOX IMVI melanoma, OVCAR-8 ovarian, and MCF-7 breast cancer cell line, being able to induce total growth inhibition (TGI) and 50% lethality (LC_{50}) at submicromolar concentrations.

Table 6. TGI and LC_{50} values (μM) of compounds **6f** and **7b** over the most sensitive cell lines.

Cancer type	Cell line	6f		7b	
		TGI	LC_{50}	TGI	LC_{50}
Leukemia	K-562	0.55	>100	- ^b	>100
	MOLT-4	0.74	>100	8.56	>100
	SR	0.55	>100	4.46	>100
	HCC-2998	0.57	2.62	3.16	- ^b
Colon	HCT-116	0.32	0.6	3.17	6.18
	SW-620	0.38	0.74	3.5	7.12
CNS	U251	0.33	0.61	3.14	5.9
Melanoma	LOX IMVI	0.42	0.89	3.57	- ^b
	M14	0.47	1.24	3.63	7.2
Ovarian	UACC-257	0.46	1.09	4.76	28.9
	OVCAR-8	0.41	0.8	4.48	- ^b
Breast	MCF7	0.43	0.99	3.43	- ^b
	MDA-MB-231/ATCC	1.96	5.38	3.98	- ^b

^a Bold figures refer to sub-micromolar TGI and LC_{50} values.

^b ND: not determined

2.2.3. *In vitro* cytotoxic activities

against HFF-1 cell line panel

To get insights about the differential cytotoxicity of this novel series of compounds, representative examples of the potent compounds **6f** and **7b** have been tested against the human foreskin fibroblast (HFF-1) normal cell utilizing MTT assay (Table 7).

Interestingly, both compounds **6f** and **7b** showed high GI_{50} values ($> 10.0 \mu\text{M}$), which reveal their selective cytotoxic activities towards human cancer cells rather normal cell lines.

Table 7. Cytotoxicity evaluation of compounds **6f** and **7b** against the HFF-1 normal cell line.

Compound No.	% growth inhibition at 10 μ M	GI ₅₀ (μ M)	2.3. <i>In vitro</i> kinase screening
6f	14.12	> 10.0	Aiming at investigation of the mechanism of action of this new series of compounds and its kinase inhibitory profile, compound 6f , the most active member, was tested at 10 μ M concentration over a panel of 53 oncogenic kinases at Reaction Biology Corporation (RBC, Malvern, PA, USA) [28]. As shown in Figure 5, compound 6f displayed highly potent inhibitory activity (above 95%) against three kinases; Tie-2 (97.4%), TrkA (95.3%) and FGFR4 (95.3%). Moreover, it exerted good inhibitory activity (70.3%–85.2%) towards FMS, IGFIR and LYN kinases, and moderate activity against FGFR1 (57.4%), FGFR3 (39.2%) and Yes-1 (45.5%). Meanwhile, it showed modest activity against the other kinases with inhibition percentage less than 35.
7b	15.77	> 10.0	

its kinase inhibitory profile, compound **6f**, the most active member, was tested at 10 μ M concentration over a panel of 53 oncogenic kinases at Reaction Biology Corporation (RBC, Malvern, PA, USA) [28]. As shown in Figure 5, compound **6f** displayed highly potent inhibitory activity (above 95%) against three kinases; Tie-2 (97.4%), TrkA (95.3%) and FGFR4 (95.3%). Moreover, it exerted good inhibitory activity (70.3%–85.2%) towards FMS, IGFIR and LYN kinases, and moderate activity against FGFR1 (57.4%), FGFR3 (39.2%) and Yes-1 (45.5%). Meanwhile, it showed modest activity against the other kinases with inhibition percentage less than 35.

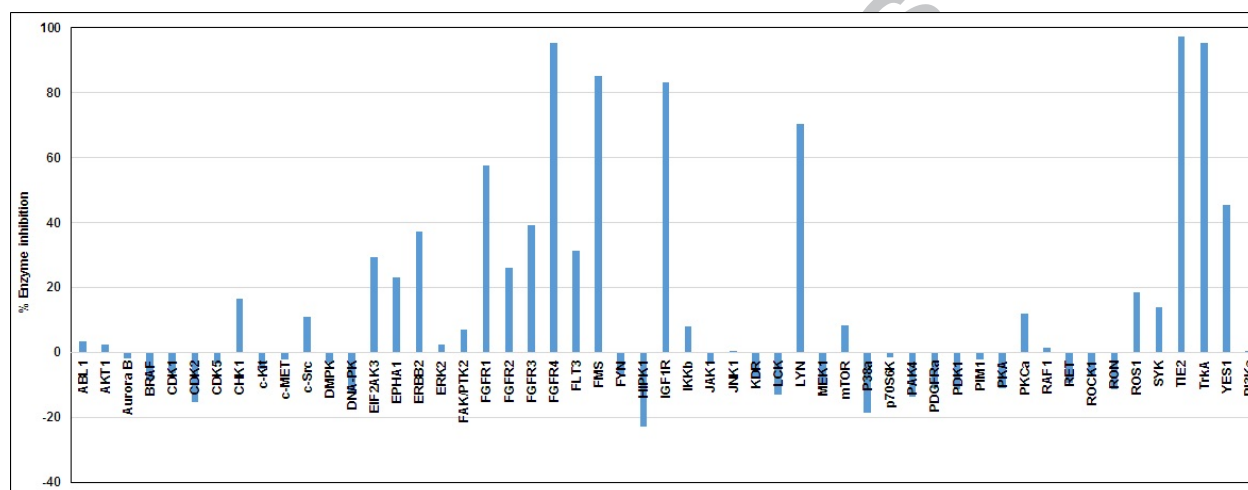


Figure 5. Inhibition percentages of compound **6f** over a panel of 53 oncogenic protein kinases at 10 μ M concentration.

Since compound **6f** displayed distinct activity against FGFR4, it was interesting to further examine the kinase inhibitory activity of the relevant derivatives **6d**, **6e**, **6g** and **7b** over the four subtypes of FGFR (Table 8). As revealed from the results, all the tested pyrrolopyrimidine octamides **6d**, **6e**, **6g** exerted moderate activity (about 50%) towards FGFR1 which is comparable to that of **6f**. In contrast, the 2-amino pyrrolopyrimidine **7b** did not possess any inhibitory activity against FGFR1. Furthermore, all compounds showed relatively weak inhibition over FGFR2, FGFR3 and FGFR4 except **6f** and **7b** which exhibited particular selectivity towards FGFR4 kinase.

Table 8. *In vitro* enzymatic inhibitory activity of **6d–g** and **7b** over the four isozymes of FGFR kinase.^a

Compound / Kinases	% Enzyme inhibition (relative to DMSO controls) (10 μ M)			
	FGFR1	FGFR2	FGFR3	FGFR4
6d	47.1	24.04	34.62	27.47 ^b
6e	59.83	22.99	39.95	31.49 ^b
6f	54.45	25.93	39.22	95.38
6g	50.52	14.67	31.68	30.74 ^b
7b	-8.65	-0.49	6.1	53.17

IC ₅₀ (M)	3.70E-09	1.63E-09	1.41E-08	9.73E-08	^a
Staurosporine					Compound s were

tested in single dose duplicate mode at a concentration of 10 μ M.

^b Compound was tested in in single dose duplicate mode at a concentration of 11.1 μ M.

Encouraged by the promising results of single dose biochemical screening, we further tested the most active compounds in cell based assay (**6d–g** and **7b**) in a 10-dose testing mode to determine their IC₅₀ values over FGFR4, Tie2 and TrkA kinases (Table 9). While the four tested octamides **6d–6g** showed reasonable and comparable activity (average IC₅₀ values = 7.0 μ M) against FGFR4 and Tie2 kinases, they exerted three times remarkable activity against TrkA (average IC₅₀ values = 2.5 μ M). It seems that the position of fluorine group has marginal contribution on the kinase activity against TrkA. Among the three fluoro substituted derivatives, compound **6f** was the most potent member with IC₅₀ value of 2.25 μ M against TrkA. Interestingly, the free amine **7b** was found to possess weak activity towards all three tested kinases with IC₅₀ values more than 12 μ M, which points out the significance of the lipophilic octamide moiety for retaining the kinase inhibitory activity.

Table 9. IC₅₀ (μ M) values of **6d–g** and **7b** against FGFR4, Tie2/Tek and TrkA kinases.

Compound / Kinases	IC ₅₀ (μ M) ^a			
	FGFR4	Tie2/Tek	TrkA	
6d	7.05	8.69	2.29	^a Compounds were tested in a 10-dose IC ₅₀ mode with 3-fold serial dilution using 10 μ M ATP. In agreement with the above mentioned biochemical assay
6e	7.67	5.80	3.15	
6f	6.71	6.84	2.25	
6g	7.57	8.21	2.76	
7b	26.3	24.8	12.4	
IC ₅₀ (M) Staurosporine	0.0973	0.0595	< 0.001	

findings, compound **6f** exerted high potencies over numerous cell lines belonging to TrkA correlated cancer types, like colon [29], melanoma [30] ovarian [31] and breast cancers [32]. However, the moderate potency **6f** against TrkA (IC₅₀ = 2.25 μ M) cannot justify its broad spectrum antiproliferative activity over multiple cancer cell lines. Therefore, TrkA inhibition can be one of the mechanisms by which compound **6f** displays its antiproliferative activity, with the possibility of presence of additional underlying mechanisms that contribute to this strong anticancer effect.

2.4. Molecular docking study

In order to rationalize the observed FGFR4, TIE2, and TrkA kinase inhibitory activity from a three dimensional (3D) structural perspective, **6f**, **7b**, and staurosporine were docked in the kinase domain. Figure 6 illustrates the 3D-interaction model of **6f** with FGFR4, TIE2, and TrkA, while the corresponding 2D interaction model is shown in Supplementary Figure 1. The docking model demonstrates that **6f** was located deep inside the extended hydrophobic pocket formed by the DFG out conformation and α C-helix region in FGFR4, TIE2, and TrkA. Glide docking score of **6f** inside FGFR4, TIE2, and TrkA is -7.01 , -6.77 , and -7.08 kcal/mol, respectively. In FGFR4 (Figure 6A), piperazine, pyrrole, and pyrimidine rings of **6f** were involved in salt-bridge and π -anion interactions

with Asp630 of DFG motif. The Cys608 forms conventional hydrogen bond with piperazine rings protonated NH and π -alkyl interactions with *m*-fluorobenzyl moiety. Another *m*-fluorobenzyl moiety forms alkyl interactions with Arg635 and Ile640, and π -anion interaction with Asp516 of α C-helix. Furthermore, octamide docked nearby the hinge region and interacted with the Val550, Glu551, and Ala553. Referring to the docking model of **6f** inside TIE2 (Figure 6B), Lys855 was involved in hydrogen-bond and π -cationic interaction with octamide and central pyrrole and pyrimidine moiety. Asp982 in DFG motif forms salt-bridge with one of the protonated nitrogen in piperazine ring. Moreover, Glu872 and Asp868 of α C-helix forms salt-bridge and hydrogen-bond interactions with both the protonated nitrogens in piperazine ring, respectively. Val875 and Arg963 form π -alkyl and hydrogen-bond interaction with *m*-fluorobenzyl moiety. In addition, the octamide moiety was found to be penetrated into the pocket formed by the hinge region (Tyr904, and Ala905). Docked model of **6f** inside TrkA is shown in Figure 6C. The nitrogen of pyrrole ring was engaged in a hydrogen bond interaction with Glu560 of α C-helix. Moreover, Leu563 and Leu564 of α C-helix formed hydrophobic interactions with the pyrimidine moiety. Furthermore, the terminal part of octamide appeared to make close contacts *via* π -alkyl and alkyl interactions with Leu657 and Phe669, respectively. Also, **6f** appeared to form close van der Waals contact with various amino acid residues (like Val524, Lys544, Leu546, Leu563, Val573, Phe589), and gatekeeper Phe589. Besides, salt bridge (ionic) interactions were formed between the protonated nitrogen of both piperazinyll moieties and Asp668 of DFG motif, and Glu560 of α C-helix. Moreover, the fluorine of *m*-fluorobenzyl was involved in halogen bond with the Phe521 residue of glycine-rich loops in the DFG-out conformation.

Additional docking experiments were carried out for **7b**, which has glide docking score of -5.08 , -5.52 , and -5.73 kcal/mol against FGFR4, TIE2, and TrkA, respectively. From the docking mode of **7b** inside FGFR4, TIE2, and TrkA (Supplementary Figures 2 and 3), it is evident that the octamide chain is necessary to improve the binding affinity. The docking model of **7b** inside FGFR4 (Supplementary Figure 2A) shows that in the absence of octamide chain, **7b** is devoid of any interaction with the hinge region, but interacts with the gatekeeper Val550. Asp630 from DFG motif is engaged with the central pyrrole and pyrimidine ring through π -anion interaction. Met524, Ile534, Leu619, Ala629, and Phe631 interact with *m*-dichlorobenzene *via* π -alkyl interactions. The chlorine of another *m*-dichlorobenzene is involved in alkyl interaction with Leu526. Glu520 and Met524 of α C-helix form salt-bridge and hydrogen bond interactions with protonated nitrogen of piperazine, respectively. Regarding the binding mode of **7b** inside TIE2 (Supplementary Figure 2B), Asp982 from DFG motif makes strong attractive charge interaction with the protonated nitrogen of piperazine ring. Also, Asp868 and Glu872 from α C-helix engage *via* salt bridge interaction with the single and double piperazine of **7b**, respectively. Moreover, Ile886 from the activation loop, Leu876, Leu879 from α C-helix and Phe960, His962, and Arg963 form π -alkyl, hydrogen bond, and π -sigma interactions with *m*-dichlorobenzene and the pyrimidine ring. Upon investigation of the docking model of **7b** into TrkA kinase (Supplementary Figure 2C), it was observed that Asp668 from DFG

motif makes a salt bridge and π -anion interactions with the protonated nitrogen and pyrrole ring. Asp556 and Glu560 residues, from α C-helix, were engaged with protonated nitrogen of piperazine moieties through single and double salt bridge interactions, respectively. Furthermore, α C-helix Leu564 and Leu567, Ile572, Val573, Leu641, Phe646 and gatekeeper Phe589 were involved in alkyl and π -alkyl interactions with *m*-dichlorobenzene. Moreover, another *m*-dichlorobenzene shared π -alkyl interactions with Ser552 and Ala553 from α C-helix, and halogen and alkyl interactions with the Phe521 and Leu546 from lysine-rich loop.

On the other hand, staurosporine was docked inside FGFR4, TIE2 and TrkA with the glide docking score of -3.45 , -5.88 , and -11.48 kcal/mol, respectively. The docking model of staurosporine is depicted in the Supplementary Figure 4. The putative binding mode of staurosporine inside FGFR4 showed hydrogen bond and π -anion interactions between DFG (Asp630) and α C-helix (Glu520) with pyrrolidone moiety. Val523 and Cys608 were engaged with staurosporine *via* π -sigma and π -sulfur interactions. Staurosporine exhibited van der Waals interactions with Phe478, Lys503, Ile527, Phe631, Gly632, Leu633, and Arg635. The docked model of staurosporine with TIE2 (Supplementary Figure 4B) exhibited van der Waals and hydrogen bond interactions with the gatekeeper (Ile902), and hinge region (Glu903, Tyr904, and Ala905), respectively. The pyrrolidone rings oxygen formed a hydrogen bond with the main chain of Ala905. In addition, the methoxy group of staurosporine interacted through π -sigma interactions with DFG motif (Phe983). Moreover, Asp912 from α C-helix participated *via* salt bridge interaction with the protonated nitrogen of staurosporine. Ala853 and Val838 shared π -alkyl and π -sigma interactions with staurosporine. The docking mode of staurosporine inside TrkA (Supplementary Figure 4C) exhibited strong hydrogen bonds, π -sigma, and salt bridge interaction network, which resulted in higher glide docking score for staurosporine. Two hydrogen bonds are formed between the hinge region residues (Glu590 and Met592) and pyrrolidone rings NH and C=O. Additionally, gatekeeper residue (Phe589) and DFG motif (Phe669) shared π - π T-shaped and stacked interactions. Asp596 from α D-helix participated in salt bridge interactions with the protonated *N*-Met. Moreover, Leu516, Val524, and Leu657 from β 1, β 2 sheet and catalytic loop formed π -alkyl and π -sigma interactions. Also, Ala542 and Met671 forms π -alkyl and alkyl interactions and Gly517, Lys544, Val573, Tyr591, Gly595, Ser672, Ile675, and Tyr676 interacted through van der Waals interactions.

Surprisingly, **6f** did not show any binding interaction with the hinge region residues in TrkA but it showed alkyl interactions in FGFR4 and TIE2. Additional alkyl interaction of **6f** from hinge region residues in FGFR4 and TIE2 did not benefit concerning docking score. Our observation is following the previous report suggesting that specific kinase inhibitors exert their activities through binding to the juxtamembrane (JM) region, a critical activity-controlling segment of receptor tyrosine kinases (RTKs), rather than hinge region [33]. Compound **7b** without octamide resulted in barren of any interactions with the hinge region and directly affects the docking score against FGFR4, TIE2, and TrkA. This observation implies that octamide is necessary to maintain the activity. Furthermore,

reference compound staurosporine showed dramatic increase in the glide docking score against TrkA compared with TIE2, and FGFR4. A putative binding model showed that staurosporine could form two hydrogen bond between pyrrolidone ring and hinge region residues (Glu590 and Met592) inside TrkA, and one hydrogen bond with Ala905 inside TIE2, and no hydrogen bond in FGFR4. Such observation suggests that for a ligand to become highly potent kinase inhibitors, it is essential to form the critical hydrogen bonds with the hinge region of kinases. Though, **6f** could participate in alkyl interactions with the hinge regions of FGFR4 and TIE2, still it is less active because it does not fulfill the criterion of a hydrogen bond with hinge region. Taken together, we can conclude that the structural features of **6f** allow profitable binding with TrkA kinase. Also, it could be suggested that **6f** might be a type III kinase inhibitor which lacks any interaction with the hinge region but binds to an allosteric pocket formed by DFG-out conformation and α C-helix region.

Beside the aforementioned docking studies for the active compounds **6f** and **7b**, further docking investigations were performed for compounds **6b**, **7e**, and **7f** to get some structural insights about their lack of antiproliferative effects. Compound **6b** was found to be unable to dock into the binding pockets of FGFR4, TIE2 and TrkA, suggesting that combining both 3,5-dichloro-phenyl with octamide moiety in single molecule is detrimental for the activity, because the 3D-shape obtained by **6b** could not be complementary to fit into the binding pocket. Docking results of compound **7e**, and **7f** suggests that the octamide moiety is critical for the activity as it extend into the ATP binding site near hinge region and forms van der Waals contact with the surrounding residues.

The docking models of **7e** and **7f** inside FGFR4 (Supplementary Figure 5A, B) showed docking scores of -4.71 kcal/mol and -4.80 kcal/mol, respectively. Piperazinyl moieties of the **7e** retain the salt bridge interactions with the Asp516 and Glu520 of α C-helix, respectively. In absence of octamide moiety, **7e** interacts with the allosteric pocket including Asp630 from DFG motif. In case of compound **7f**, different orientation in the pocket was observed. Piperazinyl moieties retain the salt-bridge interaction with the Glu520 of α C-helix and Asp630 of DFG motif. Asp516 shows the pi-cation interactions with the fused ring structure. This compound is devoid of any interaction with the hinge region and this could be the probable reason for its inactivity against FGFR4.

Docking models of **7e** and **7f** inside TIE2 are shown in Supplementary Figure 5C, D. Unlike FGFR4, neither **7e** nor **7f** interacts near hinge region of TIE2. Docking score for **7e** and **7f** are -4.71 kcal/mol and -4.55 kcal/mol, respectively. They bind into the allosteric pocket formed by DFG motif, α C-helix, and β 2- β 3 strands. One of the piperazine moiety of **7e** could form attractive charge interaction with Asp868, and Glu872 from α C-helix. The other piperazine moiety interacts with DFG motif's Asp982. Substitution on the benzyl ring (2-F vs 3-F) leads to change in the orientation of respective functional groups inside the allosteric pocket, while keeping conserved salt bridge interactions maintained. **7f** docking model also shows the salt bridge interactions with Asp868, and Glu872 of α C-helix and piperazinyl moiety. Asp982 from DFG motif shows salt-bridge interaction with the

piperazine and pi-anion interactions with central pyrrolopyrimidinone. 3F-phenyl shows halogen bond interaction with the Ile886, amide-pi stacked interaction with Ala981.

In the absence of octamide moiety in compounds **7e** and **7f**, docking modes inside TrkA (Supplementary Figure 5E, F) suggest that **7e** and **7f** docked nearby allosteric pocket but missed the interactions with hinge region. It can be seen from the **7e** docked model that both the piperazinyl moiety makes the salt-bridge interaction with the Glu556 and Asp560 of α C-helix. Overall, the ligand was reoriented in the binding pocket and became devoid of any interactions with the hinge region. The docked model of **7f** inside TrkA shows the similar interaction patterns as that of the **7e**, and piperazinyl moieties show salt-bridge interactions with the Asp556 and Glu560 of α C-helix. 3-F-phenyl moieties showed π - π stacking interactions with Phe521 from P-loop and Phe589 from gatekeeper. Docking score for the **7e** and **7f** are -4.43 kcal/mol and -4.51 kcal/mol, respectively. 2D-interaction images were shown in Supplementary Figure 6.

To become potent ATP competitive inhibitors for the kinases, small molecules need to form hydrogen-bond as well as other interactions with the hinge region. In the current study, absence of octamide substituent in compounds **7e** and **7f** makes them inactive because they miss the essential interactions with the surrounding environment of hinge region. Despite absence of octamide moiety, 3,5-dichlorophenyl piperazinyl compound **7b** showed considerable growth inhibition, but kinase inhibitory activity **7b** was low as deduced from 3D-binding mode in docking study devoid of interaction with hinge region and lower glide docking score than **6f**. Also, 3,5-dichlorophenyl piperazinyl compound **6b** having octamide moiety could not be complementary to fit in the binding pocket of FGFR4, TIE2 and TrkA, as revealed from the docking study, and displayed no enzyme activity as well.

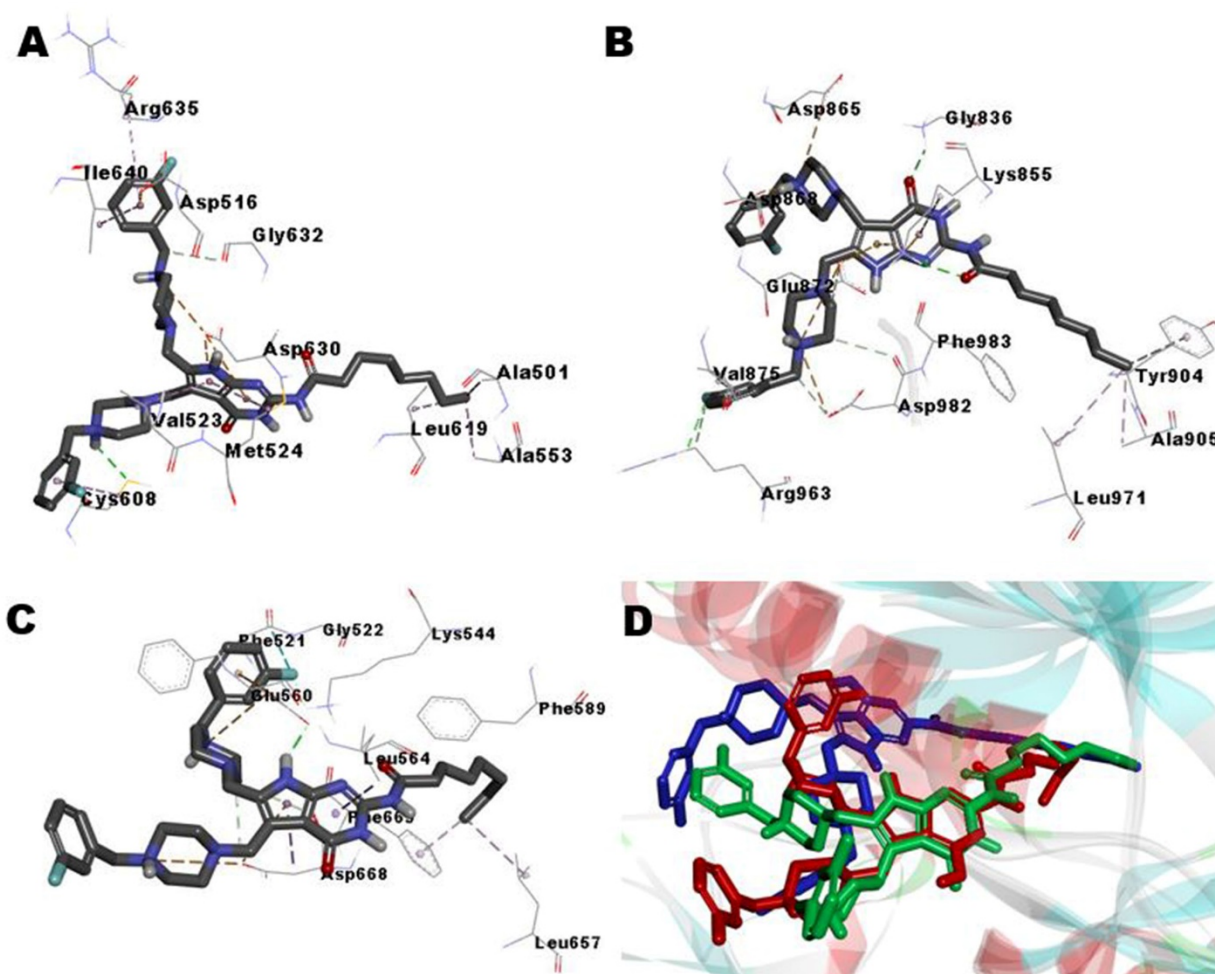


Figure 6. Docking model of **6f** inside (A) FGFR4, (B) TIE2, and (C) TrkA. For clarity purpose, only residues having interactions were shown. **6f** is shown in stick model and surrounding residues were shown in line model. Various interactions are shown in dashes. (For more clarity see the supplementary figure 1). (D) Superposed model of **6f** shown by green, blue, and red inside FGFR4, TIE2, and TrkA, respectively.

2.5. *In vivo* pharmacokinetic properties of **6f**.

The *in vivo* pharmacokinetic (PK) properties of compound **6f** were evaluated (Table 10). The AUC_{∞} values of compound **6f** are 29.9 ± 5.8 $\mu\text{g} \cdot \text{min}/\text{mL}$ and 3.7 ± 0.7 $\mu\text{g} \cdot \text{min}/\text{mL}$ in intravenous and oral administration, respectively. **6f** was moderately distributed ($T_{\max} = 2.25$ h) to reach the blood after oral administration. Moreover, it showed oral bioavailability (F) value of 12.3%.

Table 10. Pharmacokinetic parameters after intravenous ($n=3$) and oral ($n=4$) administration (10 mg/kg) of **6f** to male rats.

	Intravenous	Oral	
$AUC_{0-\infty}$ ($\mu\text{g} \cdot \text{min}/\text{ml}$)	29.9 ± 5.8	3.7 ± 0.7	The values are presented as mean \pm SD. SD, standard deviation; AUC (area under the plasma concentration
AUC_{last} ($\mu\text{g} \cdot \text{min}/\text{ml}$)	19.0 ± 2.9	3.4 ± 0.5	
Terminal half-life (min)	700.1 ± 306.1	99.4 ± 21.5	
C_{\max} ($\mu\text{g}/\text{ml}$)	- ^a	0.01 ± 0.00	
T_{\max} (min)	- ^a	$135 (60-240)^{\text{b}}$	
CL (ml/min/kg)	342.4 ± 60.6	- ^a	
F (%)	12.3		

versus time curve) = dose/clearance; C_{\max} , peak plasma concentration; T_{\max} , time to reach C_{\max} ; CL, time-averaged body clearance; F , bioavailability; ^aNot determined; ^bMedian (range) for T_{\max} .

3. Conclusion

In this study, four new series of 5-substituted and 5,6-disubstituted pyrrolo[2,3-*d*]pyrimidine octamides and their corresponding amines have been synthesized through Mannich-type reaction and evaluated for their antiproliferative activities over three human cancer cells. Among them, compounds **6d–g** and **7b** have exerted strong growth inhibitory activities with one-digit micromolar GI_{50} values over the tested cell lines. A structure activity relationship (SAR) study has been made and disclosed that terminal octamide moiety at C2 as well as disubstitution with fluorobenzyl piperazines at C5 and C6 of pyrrolo[2,3-*d*]pyrimidine are the key structural features prerequisite for best anticancer activity. The most active member **6f** was tested for its antiproliferative activity over a panel of 60 cancer cell lines at NCI, and exhibited distinct broad spectrum anticancer activity. Kinase screening of compound **6f** over 53 cancer relevant kinases at 10 μ M showed its highly selective inhibitory effects against FGFR4, Tie2 and TrkA kinases. Further determination of IC_{50} values of **6f** showed its promising activity against TrkA kinase. Such finding was justified by of molecular docking, which also revealed that **6f** did not bind with kinase hinge region, and therefore it may be a type III kinase inhibitor. The distinguished antiproliferative activity and low toxicity profile of **6f** afford a new promising chemotherapeutic candidate that could be optimized for further development of potent anticancer agents.

4. Experimental

4.1. General

¹H and ¹³C NMR spectra were recorded on a Bruker Avance 400 or 300 MHz spectrometer, using CDCl₃, DMSO-*d*₆, or D₂O as a NMR solvent. TMS was used as the internal standard and chemical shifts (δ) are reported in parts per million (ppm) and s, d, t, and m are designated as singlet, doublet, triplet and multiplet respectively. Coupling constants (J) are reported in hertz (Hz). The reaction progress was monitored on TLC plate (Merck, silica gel 60 F254), and flash column chromatography was performed on silica gel (Merck, 230e 400 mesh) with the indicated solvent system. Solvents and liquid reagents were transferred using hypodermic syringes. All solvents and reagents were commercially available and used without further purification.

4.2. 2-Amino-3,7-dihydro-4H-pyrrolo[2,3-*d*]pyrimidin-4-one (**1**) [25]

To a suspension of bromoacetaldehyde diethyl acetal (10.4 mL, 68.98 mmol) in water (35 mL) was added concentrated hydrochloric acid (1.5 mL). The reaction mixture was stirred at 90 °C. After 30 min, the solution was cooled to room temperature, and sodium acetate (6.8 g, 82.75 mmol) was added. The mixture solution was added to a suspension of 2,6-diamino-4-pyrimidinone (10.0 g, 79.29 mmol) and sodium acetate (3.5g, 42.82 mmol) in water (75 mL). The reaction mixture was stirred at 80 °C. After 2 h, the mixture was stirred at 0 °C for 90 min. The precipitate was filtered off, and washed with a little amount of cold water and acetone to afford the title product (11.9 g, quantitative yield); ¹H

NMR (300 MHz, DMSO- d_6) δ 10.97 (s, 1H), 10.23 (s, 1H), 6.61–6.60 (m, 1H), 6.18–6.17 (m, 1H), 6.05 (s, 2H).

4.3. *N*-(4-Oxo-4,7-dihydro-3H-pyrrolo[2,3-*d*]pyrimidin-2-yl)octanamide (**2**) [26]

To a suspension of compound **1** (20.0 g, 133.21 mmol) in pyridine (133 mL) was added octanoyl chloride (68.2 mL, 399.60 mmol) at 0 °C. The reaction mixture was heated at 85 °C. After 30 min, the mixture was cooled to room temperature, and neutralized with 6.5 % NH₃ in EtOH (400 mL) at 0 °C. The dark red solution was left at room temperature for overnight. A crystalline precipitate was formed, filtered off, and washed with ethanol and ether to give the title product (17.4g, 75% yield); ¹H NMR (400 MHz, DMSO- d_6) δ 11.75 (s, 1H), 11.66 (s, 1H), 11.36 (s, 1H), 6.95 (s, 1H), 6.41 (s, 1H), 2.44(t, J = 7.4 Hz, 2H), 1.59 (t, J = 6.5 Hz, 2H), 1.28 (s, 8H), 0.87 (t, J = 6.3 Hz, 3H); ¹³C NMR (75 MHz, DMSO- d_6) δ 176.4, 157.3, 148.3, 146.6, 120.0, 104.2, 102.7, 36.4, 31.6, 28.9, 24.9, 22.5, 14.4.

4.4. *N*-(5-((Dibenzylamino)methyl)-4-oxo-4,7-dihydro-3H-pyrrolo[2,3-*d*]pyrimidin-2-yl)octanamide (**3**)

To a suspension of compound **2** (4.00 g, 14.48 mmol) in 80% aqueous acetic acid (58 mL) were added 37% formalin solution (2.17 mL, 28.95 mmol) and *N,N*-dibenzylamine (5.57 mL, 28.95 mmol). The reaction mixture was stirred at 75 °C for 24 h, and cooled to room temperature. Aqueous solution of 0.5 M hydrochloric acid (72 mL) was added to the reaction mixture at room temperature. After 30 min, this mixture was neutralized with aqueous ammonia, and the mixture was then extracted with dichloromethane. The organic layer was washed with brine, dried (Na₂SO₄), and filtered. The solvent was evaporated under reduced pressure, and the residue was purified by flash column chromatography with dichloromethane/methanol (10/1, 5/1, v/v) to obtain compound **3** (5.23 g, 74% yield); ¹H NMR (300 MHz, DMSO- d_6) δ 11.55 (s, 1H), 11.36 (br. s, 1H), 7.40 (d, J = 7.0 Hz, 4H), 7.31 (t, J = 7.3 Hz, 4H), 7.23–7.19 (m, 2H), 6.87 (s, 1H), 3.76 (s, 2H), 3.57 (s, 4H), 2.42 (t, J = 7.3 Hz, 2H), 1.57 (t, J = 6.2 Hz, 2H), 1.26 (s, 8H), 0.85 (t, J = 6.4 Hz, 3H); ¹³C NMR (75 MHz, DMSO- d_6) δ 176.4, 157.8, 148.2, 146.6, 140.2, 128.8, 128.6, 127.1, 118.0, 116.2, 103.3, 57.3, 48.8, 36.4, 31.5, 28.83, 28.81, 24.9, 22.5, 14.4.

4.5. General procedure for synthesis of compounds **4a–o**

Method A: (4a–f and 4n)

To a suspension of compound **2** (1 eq.) in 80% aqueous acetic acid (4 mL) were added 37% formalin solution (2 equiv.) and the appropriate piperazine or piperidine derivative (2 equiv.). The reaction mixture was stirred at 75 °C for 24 h, and then cooled to room temperature. Aqueous solution of 0.5 N hydrochloric acid was added at room temperature. After 30 min, this mixture was neutralized with aqueous ammonia, and the mixture was then extracted with dichloromethane. The organic layer was washed with brine, dried over Na₂SO₄, and filtered. The solvent was evaporated under reduced pressure, and the residue was purified by flash column chromatography using the appropriate elution system to afford the target compounds **4a–f** and **4n** in pure form.

Method B: (4g–m and 4o)

To a suspension of compound **3** (1.0 equiv.) in MeOH/THF (1/1) was added the proper substituted piperazine or piperidine derivative (5.0 equiv.) in sealed tube. The reaction mixture was stirred at 75 °C for 24 h, and cooled to room temperature. The mixture solvent was evaporated under reduced pressure, and the residue was purified by flash column chromatography using the appropriate elution system to produce the target compounds **4g–m** and **4o** in pure form.

4.5.1. *N*-(4-Oxo-5-((4-phenylpiperazin-1-yl)methyl)-4,7-dihydro-3H-pyrrolo[2,3-d]pyrimidin-2-yl)octanamide (**4a**)

Flash column chromatography was performed using dichloromethane/methanol (15/1, 10/1, v/v) to obtain compound **4a** (12% yield); ¹H NMR (300 MHz, DMSO-*d*₆) δ 11.74 (s, 1H), 11.70 (s, 1H), 11.39 (s, 1H), 7.19 (t, *J* = 7.9 Hz, 2H), 6.91 (d, *J* = 8.3 Hz, 2H), 6.75 (t, *J* = 7.1 Hz, 1H), 6.28 (s, 1H), 3.51 (s, 2H), 3.27 (s, 2H), 3.13 (s, 4H), 2.42 (t, *J* = 7.3 Hz, 2H), 1.57 (t, *J* = 6.3 Hz, 2H), 1.26 (s, 8H), 0.85 (t, *J* = 6.3 Hz, 3H); ¹³C NMR (75 MHz, DMSO-*d*₆) δ 176.5, 157.0, 151.5, 148.6, 146.5, 130.4, 129.3, 119.2, 115.8, 104.1, 102.4, 55.0, 52.9, 48.5, 36.3, 31.6, 28.9, 25.0, 22.5, 14.4.

4.5.2. *N*-(5-((4-Benzhydrylpiperazin-1-yl)methyl)-4-oxo-4,7-dihydro-3H-pyrrolo[2,3-d]pyrimidin-2-yl)octanamide (**4b**)

Flash column chromatography was performed using dichloromethane/methanol (40/1, v/v) to obtain compound **4b** (61% yield); ¹H NMR (300 MHz, DMSO-*d*₆) δ 11.72 (s, 1H), 11.61 (s, 1H), 11.37 (s, 1H), 7.40 (d, *J* = 7.2 Hz, 5H), 7.27 (t, *J* = 7.5 Hz, 3H), 7.16 (t, *J* = 7.3 Hz, 2H), 6.21 (s, 1H), 4.25 (s, 1H), 3.45 (s, 2H), 2.42 (t, *J* = 7.2 Hz, 6H), 2.32 (br. s, 2H+2H), 1.57 (t, *J* = 6.6 Hz, 2H), 1.26 (s, 8H), 0.85 (t, *J* = 6.4 Hz, 3H); ¹³C NMR (75 MHz, DMSO-*d*₆) δ 176.5, 157.1, 148.5, 146.4, 143.3, 130.4, 130.1, 129.0, 128.0, 127.3, 104.1, 102.3, 75.5, 54.8, 52.9, 51.8, 36.3, 31.5, 28.8, 25.0, 22.5, 14.4.

4.5.3. *N*-(5-((4-(4-Methoxyphenyl)piperazin-1-yl)methyl)-4-oxo-4,7-dihydro-3H-pyrrolo[2,3-d]pyrimidin-2-yl)octanamide(**4c**)

Flash column chromatography was performed using dichloromethane/methanol (40/1, v/v) to obtain compound **4c** (quantitative yield); ¹H NMR (300 MHz, DMSO-*d*₆) δ 11.74 (s, 1H), 11.69 (s, 1H), 11.39 (s, 1H), 6.86 (d, *J* = 6.8 Hz, 2H), 6.79 (d, *J* = 9.2 Hz, 2H), 6.28 (s, 1H), 3.67 (s, 3H), 3.51 (s, 2H), 3.01 (s, 4H), 2.43 (t, *J* = 7.4 Hz, 2H), 1.58 (t, *J* = 6.7 Hz, 2H), 1.27 (s, 8H), 0.86 (t, *J* = 6.7 Hz, 3H); ¹³C NMR (75 MHz, DMSO-*d*₆) δ 176.5, 157.0, 153.3, 148.6, 146.5, 145.9, 130.4, 117.8, 114.7, 104.1, 102.4, 55.6, 55.0, 53.0, 49.9, 36.3, 31.6, 28.9, 28.8, 25.0, 22.5, 14.4.

4.5.4. *N*-(5-((4-(3-Chlorophenyl)piperazin-1-yl)methyl)-4-oxo-4,7-dihydro-3H-pyrrolo[2,3-d]pyrimidin-2-yl)octanamide (**4d**)

Flash column chromatography was performed using dichloromethane/methanol (40/1, v/v) to obtain compound **4d** (30% yield); ¹H NMR (300 MHz, DMSO-*d*₆) δ 11.74 (s, 1H), 11.68 (s, 1H), 11.38 (s, 1H), 7.19 (t, *J* = 8.1 Hz, 1H), 6.91 (s, 1H), 6.87 (d, *J* = 8.4 Hz, 2H), 6.76 (d, *J* = 7.6 Hz, 1H), 6.28 (s, 1H), 3.51 (s, 2H), 3.17 (s, 4H), 2.43 (t, *J* = 7.3 Hz, 2H), 1.57 (t, *J* = 6.3 Hz, 2H), 1.26 (s, 8H), 0.85 (t, *J* = 6.4 Hz, 3H); ¹³C NMR (75 MHz, DMSO-*d*₆) δ 176.5, 157.1, 152.7, 148.6, 146.5, 134.3, 130.8, 130.3, 118.4, 114.9, 114.1, 104.2, 102.5, 55.0, 52.7, 48.0, 36.3, 31.6, 28.9, 28.8, 25.0, 22.5, 14.4.

4.5.5. *N*-(5-((4-(2-Cyanophenyl)piperazin-1-yl)methyl)-4-oxo-4,7-dihydro-3H-pyrrolo[2,3-d]pyrimidin-2-yl)octanamide (**4e**)

Flash column chromatography was performed using dichloromethane/methanol (40/1, v/v) to obtain compound **4e** (18% yield); ¹H NMR (300 MHz, DMSO-*d*₆) δ 11.75 (br. s, 1H), 11.70 (s, 1H), 11.39 (br. s, 1H), 7.68 (d, *J* = 7.6 Hz, 1H), 7.58 (t, *J* = 7.8 Hz, 1H), 7.14 (d, *J* = 8.2 Hz, 1H), 7.08 (t, *J* = 7.5 Hz, 1H), 6.29 (s, 1H), 3.55 (s, 2H), 3.15 (s, 5H), 2.50 (s, 3H), 2.42 (t, *J* = 7.2 Hz, 2H), 1.57 (t, *J* = 6.3 Hz, 2H), 1.26 (s, 8H), 0.85 (t, *J* = 6.1 Hz, 3H); ¹³C NMR (75 MHz, DMSO-*d*₆) δ 176.5, 157.1, 155.7, 148.6, 146.5, 134.8, 134.7, 130.2, 122.4, 119.5, 118.7, 105.2, 104.2, 102.5, 54.8, 52.8, 51.6, 36.3, 31.6, 28.8, 25.0, 22.5, 14.4.

4.5.6. *N*-(5-((4-(4-Nitrophenyl)piperazin-1-yl)methyl)-4-oxo-4,7-dihydro-3H-pyrrolo[2,3-d]pyrimidin-2-yl)octanamide (**4f**)

Flash column chromatography was performed using dichloromethane/methanol (40/1, 20/1, v/v) to obtain compound **4f** (48% yield); ¹H NMR (300 MHz, DMSO-*d*₆) δ 8.04 (d, *J* = 9.4 Hz, 2H), 7.01 (d, *J* = 9.5 Hz, 2H), 6.28 (s, 1H), 3.53 (s, 2H), 3.46 (s, 4H), 2.43 (t, *J* = 7.4 Hz, 2H), 1.58 (t, *J* = 6.3 Hz, 2H), 1.27 (s, 8H), 0.86 (t, *J* = 6.4 Hz, 3H); ¹³C NMR (75 MHz, DMSO-*d*₆) δ 176.5, 157.1, 155.2, 148.6, 146.5, 137.3, 130.1, 126.2, 113.1, 104.2, 102.5, 54.8, 52.4, 46.7, 36.4, 31.5, 28.84, 28.80, 25.0, 22.5, 14.4.

4.5.7. *N*-(5-((4-(3-Fluorobenzyl)piperazin-1-yl)methyl)-4-oxo-4,7-dihydro-3H-pyrrolo[2,3-d]pyrimidin-2-yl)octanamide (**4g**)

Flash column chromatography was performed using dichloromethane/methanol (10/1, v/v) to obtain compound **4g** (16% yield); ¹H NMR (300 MHz, DMSO-*d*₆) δ 11.62 (br. s, 1H), 11.56 (s, 1H), 11.33 (s, 1H), 7.33 (t, *J* = 6.9 Hz, 1H), 7.12–7.02 (m, 3H), 6.79 (s, 1H), 3.72 (br. s, 2H), 3.46 (s, 2H), 2.42 (t, *J* = 7.4 Hz, 2H), 2.40 (br. s, 5H), 1.57 (t, *J* = 6.8 Hz, 2H), 1.26 (s, 8H), 0.85 (t, *J* = 6.3 Hz, 3H); ¹³C NMR (150 MHz, DMSO-*d*₆) δ 175.9, 163.0, 161.4, 157.3, 147.6, 146.1, 141.4, 130.02, 129.96, 124.6, 115.1, 115.0, 113.7, 113.5, 103.0, 61.2, 52.2, 51.8, 35.9, 31.1, 29.8, 28.3, 24.4, 22.0, 13.9.

4.5.8. *N*-(5-((4-Methylpiperazin-1-yl)methyl)-4-oxo-4,7-dihydro-3H-pyrrolo[2,3-d]pyrimidin-2-yl)octanamide (**4h**)

Flash column chromatography was performed using dichloromethane/methanol (10/1, 5/1, v/v) to obtain compound **4h** (31% yield); ¹H NMR (400 MHz, DMSO-*d*₆) δ 11.65 (br. s, 1H), 11.52 (s, 1H), 11.33 (br. s, 1H), 6.77 (s, 1H), 3.65 (s, 2H), 2.43 (t, *J* = 6.2 Hz, 6H), 2.29 (br. s, 4H), 2.13 (s, 3H), 1.59 (br. s, 2H), 1.28 (s, 8H), 0.87 (t, *J* = 6.4 Hz, 3H); ¹³C NMR (75 MHz, DMSO-*d*₆) δ 176.3, 157.7, 148.0, 146.5, 118.7, 115.3, 103.5, 55.3, 52.9, 52.4, 46.3, 36.4, 31.6, 28.8, 24.9, 22.5, 14.4.

4.5.9. *N*-(5-((1H-Imidazol-1-yl)methyl)-4-oxo-4,7-dihydro-3H-pyrrolo[2,3-d]pyrimidin-2-yl)octanamide (**4i**)

Flash column chromatography was performed using dichloromethane/methanol (20/1, 10/1, v/v) to obtain compound **4i** (40% yield); ¹H NMR (300 MHz, DMSO-*d*₆) δ 7.82 (s, 1H), 7.28 (s, 1H), 6.98 (s, 1H), 6.88 (s, 1H), 5.22 (s, 2H), 3.32 (s, 2H), 2.43 (t, *J* = 7.5 Hz, 2H), 1.58 (t, *J* = 6.2 Hz, 2H), 1.27 (s,

8H), 0.86 (t, $J = 6.4$ Hz, 3H); ^{13}C NMR (75 MHz, DMSO- d_6) δ 176.5, 157.6, 148.7, 147.1, 137.2, 127.8, 119.9, 119.5, 115.0, 102.3, 42.1, 36.4, 31.5, 28.8, 24.9, 22.5, 14.4.

4.5.10.N-(5-((4-Acetylpiperazin-1-yl)methyl)-4-oxo-4,7-dihydro-3H-pyrrolo[2,3-d]pyrimidin-2-yl)octanamide (4j)

Flash column chromatography was performed using dichloromethane/methanol/water/aq. NH_3 (80/16/1/1, v/v/v/v) to obtain compound **4j** (97% yield); ^1H NMR (300 MHz, MeOD- d_4) δ 7.91 (s, 1H), 6.77 (s, 1H), 4.07 (s, 2H), 3.69–3.66 (m, 4H), 2.93 (br. s, 2H), 2.87 (br. s, 2H), 2.23 (t, $J = 7.5$ Hz, 2H), 2.09 (s, 3H), 1.61 (t, $J = 6.9$ Hz, 2H), 1.29 (s, 8H), 0.88 (t, $J = 6.4$ Hz, 3H); ^{13}C NMR (75 MHz, MeOD- d_4) δ 170.2, 161.0, 153.0, 151.8, 118.5, 109.9, 99.1, 78.2, 52.1, 51.2, 51.0, 44.6, 39.9, 36.4, 31.6, 29.2, 28.9, 25.8, 22.3, 19.8, 13.1.

4.5.11.N-(5-((4-(Furan-2-carbonyl)piperazin-1-yl)methyl)-4-oxo-4,7-dihydro-3H-pyrrolo[2,3-d]pyrimidin-2-yl)octanamide (4k)

Flash column chromatography was performed using dichloromethane/methanol (10/1, 5/1, v/v) to obtain compound **4k** (5.4% yield); ^1H NMR (300 MHz, MeOD- d_4) δ 7.69 (s, 1H), 7.58 (s, 1H), 6.99–6.97 (m, 1H), 6.83 (s, 1H), 6.52–6.51 (m, 1H), 6.44 (s, 1H), 3.90 (s, 1H), 3.81 (br. s, 4H), 3.61 (s, 1H), 2.66 (s, 3H), 2.56 (s, 2H), 2.44 (t, $J = 7.3$ Hz, 2H), 1.69 (t, $J = 6.3$ Hz, 2H), 1.29 (s, 8H), 0.88 (t, $J = 6.3$ Hz, 3H); ^{13}C NMR (75 MHz, MeOD- d_4) δ 176.1, 159.6, 147.0, 144.4, 130.0, 119.8, 116.6, 116.5, 113.3, 111.1, 104.0, 102.3, 54.5, 52.5, 52.0, 36.5, 31.5, 28.84, 28.78, 24.9, 22.4, 13.4.

4.5.12.N-(5-((4-(2-Hydroxyethyl)piperazin-1-yl)methyl)-4-oxo-4,7-dihydro-3H-pyrrolo[2,3-d]pyrimidin-2-yl)octanamide (4l)

Flash column chromatography was performed using dichloromethane/methanol/aqueous NH_3 (40/8/1, v/v/v) to obtain the compound **4l** (13% yield); ^1H NMR (300 MHz, DMSO- d_6) δ 11.64 (br. s, 1H), 11.52 (s, 1H), 11.35 (br. s, 1H), 6.75 (s, 1H), 4.33 (br. s, 1H), 3.63 (s, 2H), 3.44 (br. s, 4H), 2.41 (s, 10H), 1.56 (br. s, 2H), 1.26 (s, 8H), 0.85 (s, 3H); ^{13}C NMR (75 MHz, DMSO- d_6) δ 176.3, 157.7, 148.0, 146.4, 118.6, 115.2, 103.5, 60.8, 59.0, 53.8, 52.9, 52.5, 36.3, 31.6, 28.8, 24.9, 22.5, 14.4.

4.5.13.N-(5-((4-(2-Morpholinoethyl)piperazin-1-yl)methyl)-4-oxo-4,7-dihydro-3H-pyrrolo[2,3-d]pyrimidin-2-yl)octanamide (4m)

Flash column chromatography was performed using dichloromethane/methanol/aqueous NH_3 (40/8/1, v/v/v) to obtain compound **4m** (14% yield); ^1H NMR (300 MHz, CD_3OD) δ 7.35 (br. s, 2H), 6.90 (s, 1H), 3.91 (s, 2H), 3.70–3.68 (m, 5H), 2.54–2.44 (m, 15H), 1.71 (t, $J = 7.5$ Hz, 2H), 1.34 (s, 8H), 0.92 (t, $J = 6.3$ Hz, 3H).

4.5.14.N-(4-Oxo-5-(piperidin-1-ylmethyl)-4,7-dihydro-3H-pyrrolo[2,3-d]pyrimidin-2-yl)octanamide (4n)

Flash column chromatography was performed using dichloromethane/methanol (25/1, 15/1, v/v) to obtain compound **4n** (30% yield); ^1H NMR (300 MHz, DMSO- d_6) δ 11.73 (s, 1H), 11.61 (s, 1H), 11.38 (s, 1H), 6.21 (s, 1H), 3.40 (s, 2H), 2.43 (t, $J = 7.4$ Hz, 2H), 2.33 (s, 4H), 1.56 (t, $J = 6.3$ Hz, 2H), 1.49 (s, 5H), 1.38 (br. s, 3H), 1.27 (s, 8H), 0.86 (t, $J = 6.4$ Hz, 3H); ^{13}C NMR (75 MHz, DMSO-

d_6) δ 176.4, 157.0, 148.5, 146.4, 130.9, 104.1, 102.1, 55.8, 54.1, 36.3, 31.5, 28.8, 25.8, 25.0, 24.4, 22.5, 14.4.

4.5.15. *tert*-Butyl(1-((2-octanamido-4-oxo-4,7-dihydro-3H-pyrrolo[2,3-d]pyrimidin-5-yl)methyl)piperidin-4-yl)carbamate (**4o**)

Flash column chromatography was performed using dichloromethane/methanol/aqueous NH_3 (40/8/1, v/v/v) to obtain compound **4o** (11% yield); ^1H NMR (300 MHz, $\text{DMSO-}d_6$) δ 11.62 (br. s, 1H), 11.50 (s, 1H), 11.30 (br. s, 1H), 6.76 (s, 1H), 3.63 (s, 2H), 3.32 (s, 2H), 3.14 (br. s, 1H), 2.84 (d, $J = 9.7$ Hz, 2H), 2.42 (t, $J = 7.0$ Hz, 2H), 1.98 (t, $J = 10.1$ Hz, 2H), 1.62–1.57 (m, 4H), 1.36 (s, 9H), 1.27 (s, 8H), 0.86 (t, $J = 6.4$ Hz, 3H).

4.6. General procedure for synthesis of compounds **5a–m**

To a solution of the appropriate octamide derivative **4** (1.0 equiv.) in MeOH/THF (1/1) was added aqueous 5 N KOH (0.25 equiv.). The reaction mixture was stirred at room temperature for 3 days. The solvent was evaporated under reduced pressure, and the residue was washed with CH_3CN and filtered, or the residue was purified with flash column chromatography using the proper eluent to afford compounds **5a–m** in pure form.

4.6.1. 2-Amino-5-((4-phenylpiperazin-1-yl)methyl)-3,7-dihydro-4H-pyrrolo[2,3-d]pyrimidin-4-one (**5a**)

81% yield; ^1H NMR (300 MHz, $\text{DMSO-}d_6$) δ 10.98 (s, 1H), 10.17 (s, 1H), 7.19 (t, $J = 7.4$ Hz, 2H), 6.91 (d, $J = 8.6$ Hz, 2H), 6.76 (t, $J = 6.7$ Hz, 1H), 6.05 (s, 1H), 6.03 (s, 2H), 3.42 (s, 2H), 3.32 (s, 4H), 3.12 (s, 4H); ^{13}C NMR (100 MHz, $\text{DMSO-}d_6$) δ 159.0, 152.6, 151.9, 151.5, 129.4, 127.2, 119.2, 115.8, 101.7, 100.2, 55.2, 52.8, 48.6.

4.6.2. 2-Amino-5-((4-benzhydrylpiperazin-1-yl)methyl)-3,7-dihydro-4H-pyrrolo[2,3-d]pyrimidin-4-one (**5b**)

66% yield; ^1H NMR (300 MHz, $\text{DMSO-}d_6$) δ 10.93 (s, 1H), 10.21 (s, 1H), 7.39 (d, $J = 7.0$ Hz, 5H), 7.26 (t, $J = 7.2$ Hz, 3H), 7.16 (d, $J = 7.1$ Hz, 2H), 6.08 (s, 1H), 6.03 (s, 1H), 4.15 (s, 1H), 2.33 (s, 4H); ^{13}C NMR (75 MHz, $\text{DMSO-}d_6$) δ 159.0, 152.7, 151.8, 143.3, 129.0, 128.0, 127.3, 100.3, 75.4, 54.7, 52.6, 51.6.

4.6.3. 2-Amino-5-((4-(4-methoxyphenyl)piperazin-1-yl)methyl)-3,7-dihydro-4H-pyrrolo[2,3-d]pyrimidin-4-one (**5c**)

60% yield; ^1H NMR (300 MHz, $\text{DMSO-}d_6$) δ 11.22 (s, 1H), 7.00 (br. s., 2H), 6.88 (d, $J = 8.9$ Hz, 2H), 6.79 (d, $J = 8.8$ Hz, 2H), 6.00 (s, 1H), 3.66 (s, 3H), 3.44 (s, 3H), 3.02 (s, 5H); ^{13}C NMR (100 MHz, $\text{DMSO-}d_6$) δ 162.4, 153.3, 146.0, 126.1, 117.8, 114.7, 101.6, 100.3, 55.6, 52.9, 50.0.

4.6.4. 2-Amino-5-((4-(3-chlorophenyl)piperazin-1-yl)methyl)-3,7-dihydro-4H-pyrrolo[2,3-d]pyrimidin-4-one (**5d**)

89% yield; ^1H NMR (300 MHz, $\text{DMSO-}d_6$) δ 11.10 (s, 1H), 7.19 (t, $J = 7.9$ Hz, 1H), 6.93 (s, 1H), 6.89 (d, $J = 9.1$ Hz, 1H), 6.76 (d, $J = 7.6$ Hz, 2H), 5.95 (s, 1H), 3.43 (s, 4H), 3.18 (s, 4H); ^{13}C NMR (75

MHz, DMSO-*d*₆) δ 166.2, 158.4, 153.7, 152.8, 134.2, 130.8, 124.8, 118.4, 115.0, 114.1, 101.7, 100.8, 55.8, 52.6, 48.0.

4.6.5. *2-(4-((2-Amino-4-oxo-4,7-dihydro-3H-pyrrolo[2,3-d]pyrimidin-5-yl)methyl)piperazin-1-yl)benzotrile (5e)*

73% yield; ¹H NMR (300 MHz, DMSO-*d*₆) δ 11.00 (s, 1H), 10.22 (s, 1H), 7.70–7.68 (m, 1H), 7.61–7.57 (m, 1H), 7.17–7.06 (m, 2H), 6.07 (s, 2H), 3.46 (s, 2H), 3.13 (s, 4H), 2.50 (s, 3H); ¹³C NMR (75 MHz, DMSO-*d*₆) δ 159.1, 155.7, 152.7, 151.8, 134.8, 134.7, 127.0, 122.4, 119.5, 118.7, 105.2, 101.8, 100.2, 54.9, 52.6, 51.6.

4.6.6. *2-Amino-5-((4-(4-nitrophenyl)piperazin-1-yl)methyl)-3,7-dihydro-4H-pyrrolo[2,3-d]pyrimidin-4-one (5f)*

Quantitative yield; ¹H NMR (400 MHz, DMSO-*d*₆) δ 11.19 (br. s, 1H), 8.03 (d, *J* = 8.7 Hz, 2H), 7.01 (d, *J* = 9.1 Hz, 3H), 5.98 (s, 1H), 3.75–3.45 (m, 10H); ¹³C NMR (100 MHz, DMSO-*d*₆) δ 164.69, 157.10, 154.81, 153.04, 136.81, 125.71, 124.59, 113.07, 112.65, 101.39, 100.07, 67.03, 55.05, 51.89, 46.19, 25.13.

4.6.7. *2-Amino-5-((4-(3-fluorobenzyl)piperazin-1-yl)methyl)-3,7-dihydro-4H-pyrrolo[2,3-d]pyrimidin-4-one (5g)*

Flash column chromatography was performed using dichloromethane/methanol/aqueous NH₃ (40/8/1, v/v/v) to afford compound **5g** (51% yield); ¹H NMR (300 MHz, MeOD-*d*₄) δ 7.33–7.25 (m, 1H), 7.10–7.04 (m, 2H), 6.97 (t, *J* = 8.4 Hz, 1H), 6.67 (s, 1H), 3.88 (s, 2H), 3.49 (s, 2H), 2.73 (br. s, 4H), 2.52 (br. s, 4H); ¹³C NMR (75 MHz, MeOD-*d*₄) δ 164.5, 161.3, 161.1, 152.9, 151.3, 140.2, 140.1, 129.6, 129.5, 124.8, 124.82, 124.78, 117.7, 115.7, 115.4, 113.8, 113.5, 111.9, 99.5, 78.1, 61.6, 52.8, 52.1, 51.9, 51.3.

4.6.8. *2-Amino-5-((4-methylpiperazin-1-yl)methyl)-3,7-dihydro-4H-pyrrolo[2,3-d]pyrimidin-4-one (5h)*

Flash column chromatography was performed using dichloromethane/methanol/aqueous NH₃ (40/8/1, v/v/v) to afford compound **5h** (73% yield); ¹H NMR (300 MHz, CD₃OD) δ 7.91 (s, 1H), 6.66 (s, 1H), 3.85 (s, 2H), 2.70 (br. s, 4H), 2.51 (br. s, 4H), 2.24 (s, 3H); ¹³C NMR (75 MHz, CD₃OD) δ 161.0, 152.9, 151.4, 117.7, 112.1, 99.5, 78.2, 53.9, 52.1, 51.1, 44.5.

4.6.9. *5-((1H-Imidazol-1-yl)methyl)-2-amino-3,7-dihydro-4H-pyrrolo[2,3-d]pyrimidin-4-one (5i)*

A solution of compound **14o** (105 mg, 0.30 mmol) in MeOH/THF (1/1) (1.5 mL) was added aqueous 5 M KOH (0.015 mL). This reaction mixture was stirred at room temperature for 3 days. The mixture was concentrated under reduced pressure, and the residue was purified by column chromatography with dichloromethane/methanol/aqueous NH₃ (40/8/1, v/v/v) to afford compound **15o** (94% yield); ¹H NMR (300 MHz, DMSO-*d*₆) δ 10.97 (s, 1H), 10.35 (br. s, 1H), 7.70 (s, 1H), 7.24 (s, 1H), 6.80 (s, 1H), 6.63 (s, 1H), 6.12 (s, 2H), 5.11 (s, 2H); ¹³C NMR (75 MHz, DMSO-*d*₆) δ 159.6, 153.0, 152.0, 137.4, 128.4, 119.7, 116.5, 114.6, 98.5, 42.2.

4.6.10. 5-((4-Acetylpiperazin-1-yl)methyl)-2-amino-3,7-dihydro-4H-pyrrolo[2,3-d]pyrimidin-4-one (**5j**)

Flash column chromatography was performed using dichloromethane/methanol/aqueous NH₃ (40/8/1, v/v/v) to afford compound **5j** (138 mg, quantitative yield); ¹H NMR (300 MHz, CD₃OD) δ 6.70 (s, 1H), 3.91 (s, 2H), 3.59 (br. s, 2H), 2.73 (br. s, 2H), 2.67 (br. s, 4H), 2.09 (s, 3H); ¹³C NMR (75 MHz, CD₃OD) δ 170.2, 160.8, 152.7, 151.5, 117.9, 111.8, 99.4, 52.1, 51.7, 51.3, 19.7.

4.6.11.2-Amino-5-((4-(2-hydroxyethyl)piperazin-1-yl)methyl)-3,7-dihydro-4H-pyrrolo[2,3-d]pyrimidin-4-one (**5k**)

Flash column chromatography was performed using dichloromethane/methanol/aqueous NH₃ (40/8/1, v/v/v) to afford the compound **5k** (58% yield); ¹H NMR (300 MHz, CD₃OD) δ 6.66 (s, 1H), 3.85 (s, 2H), 3.66 (t, *J* = 6.0 Hz, 2H), 3.36 (s, 1H), 2.70 (br. s, 4H), 2.60 (br. s, 4H), 2.52 (t, *J* = 6.0 Hz, 2H); ¹³C NMR (75 MHz, CD₃OD) δ 161.0, 152.9, 151.2, 117.7, 112.2, 99.6, 59.8, 58.4, 52.5, 52.0, 51.2.

4.6.12.2-Amino-5-((4-(2-morpholinoethyl)piperazin-1-yl)methyl)-3,7-dihydro-4H-pyrrolo[2,3-d]pyrimidin-4-one (**5l**)

Flash column chromatography was performed using dichloromethane/methanol/ aqueous NH₃ (40/8/1, v/v/v) to afford compound **5l** (43% yield); ¹H NMR (300 MHz, CD₃OD) δ 6.70 (s, 1H), 3.94 (s, 2H), 3.68 (t, *J* = 4.6 Hz, 5H), 2.80 (br. s, 4H), 2.62–2.50 (m, 11H); ¹³C NMR (75 MHz, CD₃OD) δ 161.0, 152.9, 151.5, 117.9, 111.3, 99.4, 66.2, 55.4, 54.4, 53.7, 52.2, 52.0, 51.1.

4.6.13. 2-Amino-5-(piperidin-1-ylmethyl)-3,7-dihydro-4H-pyrrolo[2,3-d]pyrimidin-4-one (**5m**)

14% yield; ¹H NMR (300 MHz, DMSO-*d*₆) δ 10.90 (s, 1H), 10.28 (br. s, 1H), 6.08 (s, 2H), 5.97 (s, 1H), 3.30 (s, 2H), 2.29 (s, 4H), 1.47 (s, 5H), 1.36 (s, 2H); ¹³C NMR (75 MHz, DMSO-*d*₆) δ 159.3, 152.8, 151.8, 127.6, 101.4, 100.1, 56.0, 54.0, 25.9, 24.5.

4.7. General procedure for synthesis of compounds **6a–g**

Compounds **6a–g** were synthesized from compound **2** following the same procedures described for compounds **4a–o**.

4.7.1. *N*-(5,6-Bis((4-benzhydrylpiperazin-1-yl)methyl)-4-oxo-4,7-dihydro-3H-pyrrolo[2,3-d]pyrimidin-2-yl)octanamide (**6a**)

Flash column chromatography was carried out using dichloromethane/methanol (40/1, 25/1, v/v) to obtain compound **6a** (10% yield); ¹H NMR (300 MHz, DMSO-*d*₆) δ 11.62 (br. s, 1H), 11.50 (s, 1H), 11.33 (br. s, 1H), 7.38 (t, *J* = 7.5 Hz, 8H), 7.30–7.23 (m, 8H), 7.20–7.12 (m, 4H), 4.23 (s, 1H), 4.15 (s, 1H), 3.66 (s, 2H), 3.47 (s, 2H), 2.41 (t, *J* = 6.7 Hz, 10H), 2.27 (br. s, 7H), 1.55 (t, *J* = 6.3 Hz, 2H), 1.24 (s, 8H), 0.84 (t, *J* = 6.1 Hz, 3H); ¹³C NMR (75 MHz, DMSO-*d*₆) δ 176.4, 157.5, 147.4, 146.3, 143.5, 143.4, 128.9, 128.8, 128.0, 127.3, 127.2, 113.2, 104.0, 75.8, 75.5, 53.2, 52.5, 52.1, 51.8, 50.9, 36.3, 31.5, 28.8, 25.0, 22.5, 14.4.

4.7.2. *N*-(5,6-Bis((4-(3,5-dichlorophenyl)piperazin-1-yl)methyl)-4-oxo-4,7-dihydro-3H-pyrrolo[2,3-d]pyrimidin-2-yl)octanamide (**6b**)

Flash column chromatography was carried out using dichloromethane/methanol (40/1, v/v) to obtain compound **6b** (34% yield); ^1H NMR (300 MHz, DMSO- d_6) δ 11.67 (s, 1H), 11.63 (s, 1H), 11.36 (s, 1H), 6.90 (d, J = 8.5 Hz, 4H), 6.82 (d, J = 6.2 Hz, 2H), 3.73 (s, 2H), 3.57 (s, 2H), 3.22 (s, 4H), 3.16 (s, 4H), 2.43 (t, J = 7.3 Hz, 2H), 1.58 (t, J = 6.6 Hz, 2H), 1.26 (s, 8H), 0.86 (t, J = 6.3 Hz, 3H); ^{13}C NMR (75 MHz, DMSO- d_6) δ 176.4, 157.5, 153.14, 153.10, 147.6, 146.5, 135.1, 135.0, 128.8, 117.3, 117.2, 113.42, 113.40, 104.0, 52.6, 52.1, 51.0, 47.7, 47.6, 36.3, 31.6, 28.8, 25.0, 22.5, 14.4.

4.7.3. *N*-(5,6-Bis((4-(4-nitrophenyl)piperazin-1-yl)methyl)-4-oxo-4,7-dihydro-3H-pyrrolo[2,3-d]pyrimidin-2-yl)octanamide (**6c**)

Flash column chromatography was carried out using dichloromethane/methanol (40/1, 20/1, v/v) to obtain compound **6c** (52% yield); ^1H NMR (300 MHz, DMSO- d_6) δ 8.03 (dd, J = 9.4 Hz, 2.1 Hz, 4H), 7.00 (t, J = 9.0 Hz, 4H), 3.75 (s, 2H), 3.59 (s, 2H), 3.46 (s, 5H), 3.40 (s, 6H), 2.42 (t, J = 7.4 Hz, 2H), 1.57 (t, J = 6.3 Hz, 2H), 1.27 (s, 8H), 0.86 (t, J = 6.4 Hz, 3H); ^{13}C NMR (75 MHz, DMSO- d_6) δ 176.4, 157.5, 155.2, 147.6, 146.5, 137.3, 137.1, 128.8, 126.2, 113.1, 113.0, 104.0, 52.6, 52.0, 50.8, 46.9, 46.8, 36.3, 31.5, 28.8, 25.0, 22.5, 14.4.

4.7.4. *N*-(5,6-Bis((4-benzylpiperazin-1-yl)methyl)-4-oxo-4,7-dihydro-3H-pyrrolo[2,3-d]pyrimidin-2-yl)octanamide (**6d**)

Flash column chromatography was carried out using dichloromethane/methanol (40/1, 25/1, v/v) to obtain compound **6d** (9% yield); ^1H NMR (300 MHz, DMSO- d_6) δ 11.62 (br. s, 1H), 11.33 (br. s, 1H), 11.28 (s, 1H), 7.24–7.17 (m, 10H), 3.67 (s, 2H), 3.48 (s, 2H), 3.42 (s, 2H), 3.38 (s, 2H), 2.41–2.37 (m, 18H), 1.57 (t, J = 6.7 Hz, 2H), 1.25 (s, 8H), 0.84 (t, J = 6.4 Hz, 3H); ^{13}C NMR (75 MHz, DMSO- d_6) δ 176.1, 157.9, 157.6, 148.1, 147.5, 146.5, 146.3, 138.71, 138.66, 138.5, 129.1, 129.0, 128.7, 128.31, 128.28, 127.1, 127.0, 118.4, 115.1, 113.3, 104.0, 103.6, 62.73, 62.67, 53.2, 53.1, 53.0, 52.8, 52.4, 51.1, 36.4, 31.6, 28.91, 28.89, 25.1, 22.5, 14.3; HRMS (ESI-TOF) m/z calcd for $\text{C}_{38}\text{H}_{53}\text{N}_8\text{O}_2$ $[\text{M}+\text{H}]^+$: 653.4291, found: 653.4291.

4.7.5. *N*-(5,6-Bis((4-(2-fluorobenzyl)piperazin-1-yl)methyl)-4-oxo-4,7-dihydro-3H-pyrrolo[2,3-d]pyrimidin-2-yl)octanamide (**6e**)

Flash column chromatography was carried out using dichloromethane/methanol (10/1, 5/1, v/v) to obtain compound **6e** (15% yield); ^1H NMR (300 MHz, DMSO- d_6) δ 11.48 (s, 1H), 11.36 (br. s, 1H), 7.39–7.24 (m, 4H), 7.18–7.08 (m, 4H), 3.64 (s, 2H), 3.49 (s, 2H), 3.46 (s, 4H), 2.43–2.31 (m, 18H), 1.56 (t, J = 6.8 Hz, 2H), 1.25 (s, 8H), 0.84 (t, J = 6.3 Hz, 3H); ^{13}C NMR (75 MHz, DMSO- d_6) δ 176.3, 162.8, 159.6, 157.5, 147.5, 146.4, 131.92, 131.86, 129.5, 129.4, 129.3, 128.8, 125.2, 125.1, 125.0, 124.9, 124.5, 115.7, 115.6, 115.4, 113.3, 103.9, 54.9, 54.2, 53.1, 52.7, 52.4, 51.0, 45.9, 36.3, 31.6, 28.8, 25.0, 22.5, 14.4; HRMS (ESI-TOF) m/z calcd for $\text{C}_{38}\text{H}_{51}\text{FN}_8\text{O}_2$ $[\text{M}+\text{H}]^+$: 689.4103, found: 689.4110.

4.7.6. *N*-(5,6-Bis((4-(3-fluorobenzyl)piperazin-1-yl)methyl)-4-oxo-4,7-dihydro-3H-pyrrolo[2,3-d]pyrimidin-2-yl)octanamide (**6f**)

Flash column chromatography was carried out using dichloromethane/methanol (40/1, 20/1, 10/1, v/v) to obtain compound **6f** (70% yield); ^1H NMR (300 MHz, DMSO- d_6) δ 11.59 (s, 1H), 11.52 (s, 1H), 11.35 (s, 1H), 7.37–7.28 (m, 2H), 7.12–7.00 (m, 6H), 3.65 (s, 2H), 3.48–3.41 (m, 6H), 2.43–2.38 (m, 17H), 1.55 (t, $J = 5.9$ Hz, 2H), 1.24 (s, 8H), 0.84 (t, $J = 6.4$ Hz, 3H); ^{13}C NMR (75 MHz, DMSO- d_6) δ 176.3, 164.3, 161.1, 147.5, 146.5, 142.1, 142.0, 141.9, 130.5, 130.4, 128.9, 125.1, 115.6, 115.4, 114.2, 113.9, 103.9, 61.7, 53.1, 52.9, 52.4, 51.1, 36.3, 31.6, 28.8, 25.0, 22.5, 14.4; HRMS (ESI-TOF) m/z calcd for $\text{C}_{38}\text{H}_{51}\text{FN}_8\text{O}_2$ $[\text{M}+\text{H}]^+$: 689.4103, found: 689.4106.

4.7.7. *N*-(5,6-Bis((4-(4-fluorobenzyl)piperazin-1-yl)methyl)-4-oxo-4,7-dihydro-3H-pyrrolo[2,3-*d*]pyrimidin-2-yl)octanamide (**6g**)

Flash column chromatography was carried out using dichloromethane/methanol (40/1, 25/1, v/v) to obtain compound **6g** (18% yield); ^1H NMR (300 MHz, DMSO- d_6) δ 11.46 (s, 1H), 7.32–7.25 (m, 4H), 7.14–7.06 (m, 4H), 3.65 (s, 2H), 3.48 (s, 2H), 3.40 (d, $J = 9.2$ Hz, 4H), 2.67 (t, $J = 4.8$ Hz, 1H), 2.44–2.27 (m, 16H), 1.57 (t, $J = 6.3$ Hz, 2H), 1.25 (s, 8H), 0.83 (t, $J = 6.4$ Hz, 3H); ^{13}C NMR (75 MHz, DMSO- d_6) δ 176.1, 163.2, 160.0, 157.6, 147.5, 146.3, 134.8, 134.7, 134.6, 130.8, 130.7, 128.7, 115.2, 114.9, 113.3, 104.0, 62.5, 61.7, 54.3, 53.1, 52.9, 52.4, 51.1, 46.0, 36.4, 31.6, 28.9, 25.1, 22.5, 14.3; HRMS (ESI-TOF) m/z calcd for $\text{C}_{38}\text{H}_{51}\text{FN}_8\text{O}_2$ $[\text{M}+\text{H}]^+$: 689.4103, found: 689.4107.

4.8. General procedure for synthesis of compounds **7a–g**

Compounds **7a–g** were synthesized from their corresponding octamides **6a–g** following the same procedures described for compounds **5a–m**.

4.8.1. 2-Amino-5,6-bis((4-benzhydrylpiperazin-1-yl)methyl)-3,7-dihydro-4H-pyrrolo[2,3-*d*]pyrimidin-4-one (**7a**)

Flash column chromatography was carried out using dichloromethane/methanol/aqueous NH_3 (40/8/1, v/v/v) to afford compound **7a** (92% yield); ^1H NMR (400 MHz, THF- d_8) δ 7.39 (d, $J = 7.5$ Hz, 8H), 7.19 (q, $J = 7.9$ Hz, 8H), 7.12–7.08 (m, 4H), 5.89 (br. s, 2H), 4.21 (s, 1H), 4.15 (s, 1H), 3.75 (s, 2H), 3.49 (s, 2H), 2.53–2.35 (m, 16H), 1.39 (s, 2H); ^{13}C NMR (100 MHz, THF- d_8) δ 144.38, 144.10, 129.17, 129.13, 128.77, 127.58, 127.58, 127.47, 77.44, 77.13, 54.25, 53.78, 53.37, 53.03, 52.66, 30.77.

4.8.2. 2-Amino-5,6-bis((4-(3,5-dichlorophenyl)piperazin-1-yl)methyl)-3,7-dihydro-4H-pyrrolo[2,3-*d*]pyrimidin-4-one (**7b**)

63% yield; ^1H NMR (300 MHz, DMSO- d_6) δ 10.99 (br. s, 1H), 10.95 (s, 1H), 6.91–6.89 (m, 4H), 6.82 (s, 2H), 6.06 (s, 2H), 3.70 (s, 2H), 3.48 (s, 2H), 3.19 (s, 8H), 2.50 (s, 8H); ^{13}C NMR (75 MHz, DMSO- d_6) δ 159.6, 153.1, 152.7, 150.9, 135.1, 125.8, 117.3, 117.2, 113.4, 111.9, 100.1, 52.5, 52.0, 51.2, 47.6; HRMS (ESI-TOF) m/z calcd for $\text{C}_{28}\text{H}_{31}\text{Cl}_4\text{N}_8\text{O}$ $[\text{M}+\text{H}]^+$: 635.1375, found: 635.1378.

4.8.3. 2-Amino-5,6-bis((4-(4-nitrophenyl)piperazin-1-yl)methyl)-3,7-dihydro-4H-pyrrolo[2,3-*d*]pyrimidin-4-one (**7c**)

Flash column chromatography was carried out using dichloromethane/methanol/aqueous NH_3 (40/8/1, v/v/v) to afford compound **7c** (60 mg, 47% yield); ^1H NMR (300 MHz, D_2O) δ 5.54–5.49 (m, 4H),

4.75 (d, $J = 8.4$ Hz, 2H), 4.61 (d, $J = 9.2$ Hz, 2H), 1.51–1.48 (m, 4H), 1.36–1.28 (m, 3H), 1.14 (br. s, 3H), 1.07–0.99 (m, 5H), 0.95 (br. s, 4H).

4.8.4. *2-Amino-5,6-bis((4-benzylpiperazin-1-yl)methyl)-3,7-dihydro-4H-pyrrolo[2,3-d]pyrimidin-4-one (7d)*

Flash column chromatography was carried out using dichloromethane/methanol/aqueous NH_3 (40/8/1, v/v/v) to afford compound **7d** (54% yield); ^1H NMR (300 MHz, $\text{DMSO}-d_6$) δ 10.71 (s, 1H), 10.02 (s, 1H), 7.28 (s, 10H), 6.00 (s, 2H), 3.57 (br. s, 8H), 2.35 (br. s, 12H).

4.8.5. *2-Amino-5,6-bis((4-(2-fluorobenzyl)piperazin-1-yl)methyl)-3,7-dihydro-4H-pyrrolo[2,3-d]pyrimidin-4-one (7e)*

Flash column chromatography was carried out using dichloromethane/methanol/aqueous NH_3 (40/8/1, v/v/v) to afford compound **7e** (94% yield); ^1H NMR (300 MHz, CDCl_3) δ 7.35–7.24 (m, 4H), 7.14–6.99 (m, 4H), 3.83 (s, 2H), 3.60–3.55 (m, 6H), 2.69 (br. s, 4H), 2.52 (s, 12H); ^{13}C NMR (75 MHz, CDCl_3) δ 167.0, 165.1, 163.8, 157.3, 155.2, 135.9, 135.8, 133.3, 133.2, 133.0, 129.9, 127.8, 127.5, 127.4, 127.3, 127.2, 119.22, 119.18, 118.92, 118.88, 115.2, 103.8, 59.4, 58.8, 58.7, 57.1, 56.3, 56.1, 55.9, 55.5, 54.8, 48.8.

4.8.6. *2-Amino-5,6-bis((4-(3-fluorobenzyl)piperazin-1-yl)methyl)-3,7-dihydro-4H-pyrrolo[2,3-d]pyrimidin-4-one (7f)*

Flash column chromatography was carried out using dichloromethane/methanol/aqueous NH_3 (40/8/1, v/v/v) to afford the compound **7f** (73% yield); ^1H NMR (300 MHz, $\text{DMSO}-d_6$) δ 8.24 (s, 2H), 7.35–7.28 (m, 2H), 7.12–7.00 (m, 6H), 6.42 (s, 1H), 4.24 (s, 2H), 3.12 (br. s, 4H), 2.50 (s, 2H), 2.42 (br. s, 4H), 2.38 (br. s, 4H); ^{13}C NMR (75 MHz, $\text{DMSO}-d_6$) δ 164.3, 161.1, 160.6, 153.1, 152.0, 141.6, 141.5, 140.9, 140.8, 131.8, 130.6, 130.5, 130.3, 127.6, 126.4, 125.1, 125.0, 115.8, 115.7, 115.6, 115.4, 114.5, 114.2, 113.9, 106.7, 99.0, 61.7, 60.9, 52.7, 52.6, 52.3, 51.2, 51.1, 50.5, 49.5, 43.4.

4.8.7. *2-Amino-5,6-bis((4-(4-fluorobenzyl)piperazin-1-yl)methyl)-3,7-dihydro-4H-pyrrolo[2,3-d]pyrimidin-4-one (7g)*

Flash column chromatography was carried out using dichloromethane/methanol/aqueous NH_3 (40/8/1, v/v/v) to afford compound **7g** (90% yield); ^1H NMR (300 MHz, CD_3OD) δ 7.29–7.22 (m, 4H), 7.01–6.93 (m, 4H), 3.79 (s, 2H), 3.54 (s, 2H), 3.48 (s, 2H), 3.44 (s, 2H), 2.63 (br. s, 4H), 2.47 (s, 12H); ^{13}C NMR (75 MHz, CD_3OD) δ 163.78, 163.74, 161.0, 160.53, 160.49, 153.3, 151.0, 132.9, 132.8, 132.75, 132.71, 131.01, 130.99, 130.91, 130.88, 125.9, 115.0, 114.9, 114.72, 114.65, 111.5, 100.0, 61.9, 52.4, 52.2, 51.6, 50.8.

4.9. Cancer cell line screening

The Antiproliferative activities of all target compounds were investigated against the human cancer cell lines using the MTT assay. HCT-116 (Human colorectal carcinoma), MCF-7 and SK-BR3 (breast cancer cells) were supplied from the Korea Cell Line Bank (KCLB). All cell lines were grown in RPMI 1640/DMEM (Gibco BRL) supplemented with 10% (V/V) heat inactivated Fetal Bovine Serum (FBS) and maintained at 37 °C in a humidified atmosphere with 5% CO_2 . The cells (5×10^4 cells/mL)

were seeded into 96-well plate. Various concentrations of samples were added to each well in duplicate, then incubated at 37 °C with 5% CO₂ for two days where cells are in the exponential phase of growth at the time of compound addition. 15 µL of the Dye Solution (Promrga, CellTiter 96®) was added to each well, and the plate was incubated at 37 °C for up to 4 h in a humidified, 5 % CO₂ atmosphere. After incubation, 100 µL of the solubilization solution/Stop Mix (Promrga, CellTiter 96®) was added to each well. The plate was allowed to stand overnight in a sealed container with a humidified atmosphere at room temperature to completely solubilize the formazan crystals. The optical density was measured using a microplate reader (VersaMax™, Molecular Devices) with a 570 nm wavelength.

The cancer cell screening over full panel of 60 human cancer cell lines was conducted at the National Cancer Institute (NCI, Bethesda, Maryland, USA) [27] adopting the standard procedure [34].

4.10. Evaluation of cytotoxicity against the HFF-1 normal cell

To get some insights about the differential cytotoxicity of this new set of compounds, the most active members **6f** and **7b** have been tested against the human foreskin fibroblast (HFF-1) normal cell line using the (3-(4,5-dimethylthiazol-2-yl)-2,5-Diphenyltetrazolium bromide) tetrazolium (MTT) assay (Table 7). Interestingly, both compounds **6d** and **6j** showed low growth inhibitory effects as indicated by their high GI₅₀ values (>10.0 µM), which point out their selective growth inhibitory activities toward human cancer cells rather normal cell lines.

4.11. In vitro kinase screening

Kinase HotSpotSM service [28] performed by Reaction Biology Corp. (Malvern, PA, USA) was used for screening of compounds **6d–g** and **7b**. Assay protocol: In a final reaction volume of 25 µL, kinase (5–10 mU) is incubated with 25 mM Tris pH 7.5, 0.02 mM EGTA, 0.66 mg/mL myelin basic protein, 10 µM magnesium acetate and [³³P-ATP] (specific activity approx. 500 cpm/pmol, concentration as required). The reaction is initiated by the addition of the Mg-ATP mix. After incubation for 40 min at room temperature, the reaction is stopped by the addition of 5 µL of a 3% phosphoric acid solution. 10 µL of the reaction is then spotted onto a P30 filtermat and washed three times for 5 min in 75 mM phosphoric acid and once in methanol prior to drying and scintillation counting.

4.12. Molecular docking

The X-ray structure of TrkA was retrieved from the protein data bank (PDB) with 4PMM accession code, and prepared utilizing the protein preparation wizard module [35] implemented in the Schrodinger 2015 package. The protein was set in a pH 7.4, and compound **6f** was sketched using the sketching option in Maestro and converted to 3D-geometry using the Ligprep module of Schrodinger [36]. The default ligand settings were used to prepare all tautomers, and further energy minimized. The co-crystal ligand was retrieved and re-docked to ensure the reproducibility of the docking program. All minimized conformations of **6f** were docked into the putative ligand binding site using Glide's standard precision module [37] and generated 50 poses each. The docking figures were

rendered using the Discovery Studio Client 2017 R2 package. The pose with more negative docking score (-7.08 Kcal/mol) and significant interactions with TrkA was selected as the best docking pose for analysis of binding mode.

4.13. *In vivo* determination of pharmacokinetic properties of **6f**

For the *in vivo* ADME study, 8 weeks male SD rat were given a single dose of the test intravenous or oral at 10 mg/kg dose of compound **6f**. Blood sampling was done at 0, 0.03, 0.17, 0.25, 0.5, 1, 2, 4, 8, 24 h from the cannula inserted in the femoral vein. Plasma was separated from the whole blood by centrifugation and extracted with organic solution (acetonitrile). Extracts were analyzed with LC-MS/MS. Non-compartmental pharmacokinetic parameters were estimated from the profile of the concentration in plasma vs time with WinNonlin program (Pharsight, USA).

Acknowledgments

This research was supported by the Korea Institute of Science and Technology (KIST) Institutional Program (2E27870 and 2E28411) and the National Research Foundation Grant (2015R1A2A1A10054108, 2014M3C1A3051476), Republic of Korea. We would like to express our genuine gratitude and appreciation to the National Cancer Institute (NCI, Bethesda, Maryland, USA) for performing the *in vitro* anticancer evaluation of the new compounds.

Supplementary data

Supplementary data associated with this article is available.

References

- [1] A. Jemal, R. Siegel, E. Ward, T. Murray, J. Xu, M.J. Thun, Cancer statistics, 2007, CA: a cancer journal for clinicians, 57 (2007) 43–66.
- [2] V. Srivastava, H. Lee, Synthesis and bio-evaluation of novel quinolino-stilbene derivatives as potential anticancer agents, Bioorg. Med. Chem. Lett. 23 (2015) 7629–7640.
- [3] J.E. Dancey, H.X. Chen, Strategies for optimizing combinations of molecularly targeted anticancer agents, Nat. Rev. Drug Discovery 5 (2006) 649.
- [4] A. Gangjee, O.A. Namjoshi, M.A. Ihnat, A. Buchanan, The contribution of a 2-amino group on receptor tyrosine kinase inhibition and antiangiogenic activity in 4-anilinosubstituted pyrrolo [2,3-*d*] pyrimidines, Bioorg. Med. Chem. Lett. 20 (2010) 3177–3181.
- [5] A. Gangjee, S. Kurup, M.A. Ihnat, J.E. Thorpe, B. Disch, *N* 4-Aryl-6-substitutedphenylmethyl-7*H*-pyrrolo [2,3-*d*] pyrimidine-2, 4-diamines as receptor tyrosine kinase inhibitors, Bioorg. Med. Chem. 20 (2012) 910–914.
- [6] A. Gangjee, O.A. Namjoshi, J. Yu, M.A. Ihnat, J.E. Thorpe, L.A. Warnke, Design, synthesis and biological evaluation of substituted pyrrolo [2,3-*d*] pyrimidines as multiple receptor tyrosine kinase inhibitors and antiangiogenic agents, Bioorg. Med. Chem. 16 (2008) 5514–5528.

- [7] A. Gangjee, Y. Zhao, S. Raghavan, M.A. Ihnat, B.C. Disch, Design, synthesis and evaluation of 2-amino-4-*m*-bromoanilino-6-arylmethyl-7*H*-pyrrolo [2,3-*d*] pyrimidines as tyrosine kinase inhibitors and antiangiogenic agents, *Bioorg. Med. Chem.* 18 (2010) 5261–5273.
- [8] A. Gangjee, N. Zaware, S. Raghavan, J. Yang, J.E. Thorpe, M.A. Ihnat, *N* 4-(3-Bromophenyl)-7-(substituted benzyl) pyrrolo [2,3-*d*] pyrimidines as potent multiple receptor tyrosine kinase inhibitors: Design, synthesis, and *in vivo* evaluation, *Bioorg. Med. Chem.* 20 (2012) 2444–2454.
- [9] S.D. Chamberlain, J.W. Wilson, F. Deanda, S. Patnaik, A.M. Redman, B. Yang, L. Shewchuk, P. Sabbatini, M.A. Leesnitzer, A. Groy, Discovery of 4, 6-bis-anilino-1*H*-pyrrolo [2,3-*d*] pyrimidines: Potent inhibitors of the IGF-1R receptor tyrosine kinase, *Bioorg. Med. Chem. Lett.* 19 (2009) 469–473.
- [10] W. Li, S. Favelyukis, J. Yang, Y. Zeng, J. Yu, A. Gangjee, W.T. Miller, Inhibition of insulin-like growth factor I receptor autophosphorylation by novel 6-5 ring-fused compounds, *Biochem. Pharmacol.* 68 (2004) 145–154.
- [11] Y. Saito, H. Yuki, M. Kuratani, Y. Hashizume, S. Takagi, T. Honma, A. Tanaka, M. Shirouzu, J. Mikuni, N. Handa, A pyrrolo-pyrimidine derivative targets human primary AML stem cells *in vivo*, *Sci. Transl. Med.* 5 (2013) 181ra52.
- [12] F. Musumeci, A.L. Fallacara, C. Brullo, G. Grossi, L. Botta, P. Calandro, M. Chiariello, M. Kissova, E. Crespan, G. Maga, Identification of new pyrrolo [2,3-*d*] pyrimidines as Src tyrosine kinase inhibitors *in vitro* active against Glioblastoma, *Eur. J. Med. Chem.* 127 (2017) 369–378.
- [13] G. Roman, Mannich bases in medicinal chemistry and drug design, *Eur. J. Med. Chem.* 89 (2015) 743–816.
- [14] M. Yarim, M. Koksall, D. Schepmann, B. Wünsch, Synthesis and *in vitro* Evaluation of Novel Indole-Based Sigma Receptors Ligands, *Chem. Biol. Drug Des.* 78 (2011) 869–875.
- [15] M.-L. Go, J.L. Leow, S.K. Gorla, A.P. Schüller, M. Wang, P.J. Casey, Amino derivatives of indole as potent inhibitors of isoprenylcysteine carboxyl methyltransferase, *J. Med. Chem.* 53 (2010) 6838–6850.
- [16] M. Qin, S. Yan, L. Wang, H. Zhang, Y. Tian, Y. Zhao, P. Gong, Novel 6-methoxycarbonyl indolinones bearing a pyrrole Mannich base moiety as angiokinase inhibitors, *Bioorg. Med. Chem.* 25 (2017) 1778–1786.
- [17] Z. Chen, A.M. Venkatesan, C.M. Dehnhardt, S. Ayril-Kaloustian, N. Brooijmans, R. Mallon, L. Feldberg, I. Hollander, J. Lucas, K. Yu, Synthesis and SAR of novel 4-morpholinopyrrolopyrimidine derivatives as potent phosphatidylinositol 3-kinase inhibitors, *J. Med. Chem.* 53 (2010) 3169–3182.
- [18] A.K. El-Damasy, N.C. Cho, G. Nam, A.N. Pae, G. Keum, Discovery of a Nanomolar Multikinase Inhibitor (KST016366): A New Benzothiazole Derivative with Remarkable Broad-Spectrum Antiproliferative Activity, *ChemMedChem*, 11 (2016) 1587–1595.

- [19] A.K. El-Damasy, N.-C. Cho, S.B. Kang, A.N. Pae, G. Keum, ABL kinase inhibitory and antiproliferative activity of novel picolinamide based benzothiazoles, *Bioorg. Med. Chem. Lett.* 25 (2015) 2162–2168.
- [20] A.K. El-Damasy, N.-C. Cho, A.N. Pae, E.E. Kim, G. Keum, Novel 5-substituted-2-anilinoquinolines with 3-(morpholino or 4-methylpiperazin-1-yl) propoxy moiety as broad spectrum antiproliferative agents: Synthesis, cell based assays and kinase screening, *Bioorg. Med. Chem. Lett.* 26 (2016) 3307–3312.
- [21] A.K. El-Damasy, J.-H. Lee, S.H. Seo, N.-C. Cho, A.N. Pae, G. Keum, Design and synthesis of new potent anticancer benzothiazole amides and ureas featuring pyridylamide moiety and possessing dual B-Raf^{V600E} and C-Raf kinase inhibitory activities, *Eur. J. Med. Chem.* 115 (2016) 201–216.
- [22] A.K. El-Damasy, S.H. Seo, N.C. Cho, A.N. Pae, E.E. Kim, G. Keum, Design and synthesis of new 2-anilinoquinolines bearing N-methylpicolinamide moiety as potential antiproliferative agents, *Chem. Biol. Drug Des.* 89 (2017) 98–113.
- [23] A.K. El-Damasy, S.H. Seo, N.-C. Cho, S.B. Kang, A.N. Pae, K.-S. Kim, G. Keum, Design, synthesis, in-vitro antiproliferative activity and kinase profile of new picolinamide based 2-amido and ureido quinoline derivatives, *Eur. J. Med. Chem.* 101 (2015) 754–768.
- [24] J.-H. Lee, S.C. Shin, S.H. Seo, Y.H. Seo, N. Jeong, C.-W. Kim, E.E. Kim, G. Keum, Synthesis and in vitro antiproliferative activity of C5-benzyl substituted 2-amino-pyrrolo [2, 3-d] pyrimidines as potent Hsp90 inhibitors, *Bioorg. Med. Chem. Lett.* 27 (2017) 237–241.
- [25] J. Shi, R. Van de Water, K. Hong, R.B. Lamer, K.W. Weichert, C.M. Sandoval, S.R. Kasibhatla, M.F. Boehm, J. Chao, K. Lundgren, N. Timple, R. Lough, G. Ibanez, C. Boykin, F.J. Burrows, M.R. Kehry, T.J. Yun, E.K. Harning, C. Ambrose, J. Thompson, S.A. Bixler, A. Dunah, P. Snodgrass-Belt, J. Arndt, I.J. Enyedy, P. Li, V.S. Hong, A. McKenzie, M.A. Biamonte, EC144 is a potent inhibitor of the heat shock protein 90, *J. Med. Chem.* 55 (2012) 7786–7795.
- [26] H. Akimoto, E. Imamiya, T. Hitaka, H. Nomura, S. Nishimura, Synthesis of queuine, the base of naturally occurring hypermodified nucleoside (queuosine), and its analogues, *J. Chem. Soc., Perkin Trans. 1* (1988) 1637–1644.
- [27] NCI website: <https://ntp.cancer.gov/>.
- [28] Reaction Biology Corporation Web Site. Available from: www.reactionbiology.com.
- [29] A. Nakagawara, Trk receptor tyrosine kinases: a bridge between cancer and neural development, *Cancer Lett.* 169 (2001) 107–114.
- [30] V.A. Flørenes, G.M. Mælandsmo, R. Holm, R. Reich, P. Lazarovici, B. Davidson, Expression of activated TrkA protein in melanocytic tumors: relationship to cell proliferation and clinical outcome, *Am. J. Clin. Pathol.* 122 (2004) 412–420.

- [31] B. Davidson, R. Reich, P. Lazarovici, J.M. Nesland, M. Skrede, B. Risberg, C.G. Tropé, V.A. Flørenes, Expression and activation of the nerve growth factor receptor TrkA in serous ovarian carcinoma, *Clin. Cancer Res.* 9 (2003) 2248–2259.
- [32] E. Adriaenssens, E. Vanhecke, P. Saule, A. Mougel, A. Page, R. Romon, V. Nurcombe, X. Le Bourhis, H. Hondermarck, Nerve growth factor is a potential therapeutic target in breast cancer, *Cancer Res.* 68 (2008) 346–351.
- [33] N. Furuya, T. Momose, K. Katsuno, N. Fushimi, H. Muranaka, C. Handa, T. Ozawa, T. Kinoshita, The juxtamembrane region of TrkA kinase is critical for inhibitor selectivity, *Bioorg. Med. Chem. Lett.* 27 (2017) 1233–1236.
- [34] DTP Human Tumor Cell Line Screen Process https://dtp.cancer.gov/discovery_development/nci-60/methodology.htm (retrieved on 19.10.2017).
- [35] G.M. Sastry, M. Adzhigirey, T. Day, R. Annabhimoju, W. Sherman, Protein and ligand preparation: parameters, protocols, and influence on virtual screening enrichments, *J. Comput.-Aided Mol. Des.* 27 (2013) 221–234.
- [36] R.J. Lefkowitz, Identification of Adenylate Cyclase-Coupled Beta-Adrenergic Receptors with Radiolabeled Beta-Adrenergic Antagonists, *Biochem. Pharmacol.* 24 (1975) 1651–1658.
- [37] R.A. Friesner, J.L. Banks, R.B. Murphy, T.A. Halgren, J.J. Klicic, D.T. Mainz, M.P. Repasky, E.H. Knoll, M. Shelley, J.K. Perry, D.E. Shaw, P. Francis, P.S. Shenkin, Glide: A new approach for rapid, accurate docking and scoring. 1. Method and assessment of docking accuracy, *J. Med. Chem.* 47 (2004) 1739–1749.

List of captions

Table 1. *In vitro* growth inhibitory data of the 5-substituted pyrrolopyrimidinyl octamides **4a–o** against MCF-7, SK-BR-3 and HCT116 cancer cell lines.

Table 2. *In vitro* growth inhibitory data of the 2-amino-5-substituted pyrrolopyrimidinones **5a–m** against MCF-7, SK-BR-3 and HCT116 cancer cell lines.

Table 3. *In vitro* growth inhibitory data of the 5,6-Bis-substituted pyrrolopyrimidinyl octamides **6a–g** against MCF-7, SK-BR-3 and HCT116 cancer cell lines.

Table 4. *In vitro* growth inhibitory data of the 2-Amino-5,6-bis-substituted pyrrolopyrimidinones **7a–g** against MCF-7, SK-BR-3 and HCT116 cancer cell lines.

Table 5. GI₅₀ values (μM) of compounds **6f** and **7b** over NCI-60 cell line panel.

Table 6. TGI and LC₅₀ values (μM) of compounds **6f** and **7b** over the most sensitive cell lines.

Table 7. Cytotoxicity evaluation of compounds **6f** and **7b** against the HFF-1 normal cell line.

Table 8. *In vitro* enzymatic inhibitory activity of **6d–g** and **7b** over the four isozymes of FGFR kinase.

Table 9. IC₅₀ (μM) values of **6d–g** and **7b** against FGFR4, Tie2/Tek and TrkA kinases.

Table 10. Pharmacokinetic parameters after intravenous ($n=3$) and oral ($n = 4$) administration (10 mg/kg) of **6f** to male rats.

Figure 1. Examples of antiproliferative pyrrolo[2,3-*d*]pyrimidine derivatives with protein kinase inhibitory activities.

Figure 2. Certain reported Mannich bases with promising antiproliferative activities. The aminoalkyl moiety is illustrated in orange.

Figure 3. General structure of the target compounds.

Figure 4. % Growth of NCI 60 cell line panel upon treatment with compounds **6f** (upper panel) and **7b** (lower panel) at 10 μ M concentration.

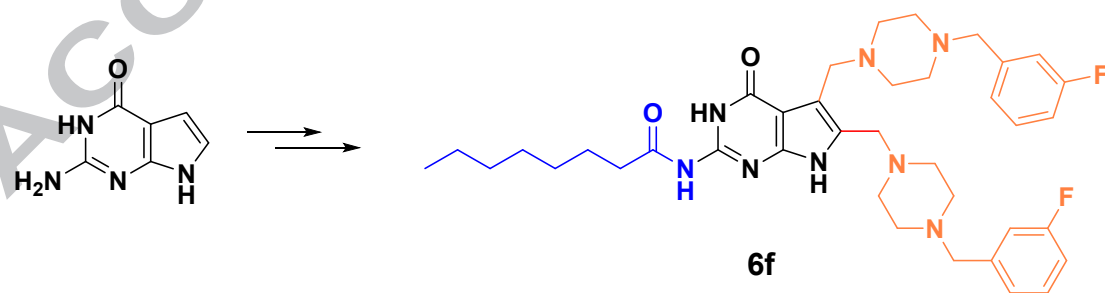
Figure 5. Inhibition percentages of compound **6f** over a panel of 53 oncogenic protein kinases at 10 μ M concentration.

Figure 6. Docking model of **6f** inside (A) FGFR4, (B) TIE2, and (C) TrkA. For clarity purpose, only residues having interactions were shown. **6f** is shown in stick model and surrounding residues were shown in line model. Various interactions are shown in dashes. (For more clarity see the supplementary figure 1). (D) Superposed model of **6f** shown by green, blue, and red inside FGFR4, TIE2, and TrkA, respectively.

Scheme 1. Reagents and reaction conditions: i) conc. HCl, NaOAc, 90 $^{\circ}$ C to rt, ii) 2,6-Diamino-4-pyrimidinone, NaOAc, 80 $^{\circ}$ C to rt, quant.; iii) Octanoyl chloride, pyridine, 85 $^{\circ}$ C, 49–75%; iv) 37% formalin, aryl piperazine, 80% AcOH, 75 $^{\circ}$ C, 12%–quant.; v) 37% Formalin, *N,N*-dibenzylamine, 80% AcOH, 75 $^{\circ}$ C, 24–74%; vi) Appropriate amines, MeOH/THF (1:1), 75 $^{\circ}$ C, 11–97%; vii) 5 M aq. KOH, MeOH/THF, rt, 60%–quant.; viii) 37% formalin, aryl or benzylpiperazine, 80% acetic acid, 75 $^{\circ}$ C, 9%–quant.

Research highlights

- Synthesis and *in vitro* antiproliferative activities of new pyrrolo[2,3-*d*]pyrimidines are reported.
- Compounds **6d–g** exerted single digit micromolar GI_{50} values over the tested cancer cell lines.
- Compound **6f** has selective inhibitory activity towards FGFR4, Tie2 and TrkA kinases.
- Compound **6f** may be a type III allosteric kinase inhibitor.



HCT-116 colon cancer; $GI_{50} = 0.17 \mu$ M, TGI = 0.32μ M
 LOX IMVI melanoma; $GI_{50} = 0.20 \mu$ M, TGI = 0.42μ M
 MCF-7 breast cancer; $GI_{50} = 0.19 \mu$ M, TGI = 0.43μ M
 FGFR4 kinase ($IC_{50} = 6.71 \mu$ M)
 TrkA kinase ($IC_{50} = 2.25 \mu$ M)